



Düzce University Journal of Science & Technology

Research Article

Dynamical simulation of a four legged robot with shooting at targets using Fuzzy Logic Control

Ahmet Burak TATAR^{a*}, Beyda TAŞAR^b, Alper Kadir TANYILDIZI^c, Oğuz YAKUT^d

^a Department of Mechanical Engineering, Faculty of Engineering, Adıyaman University, Adıyaman, TURKEY

^{b,c,d} Department of Mechatronics Engineering, Faculty of Engineering, Fırat University, Elazığ, TURKEY

* Corresponding author's e-mail address: atatar@adiyaman.edu.tr

DOI: <https://doi.org/10.29130/dubited.1114836>

ABSTRACT

This research aims to increase defense deterrence by tracking and shooting targets with a gun mounted on a quadruped robot in rough terrain and different environmental conditions. The dynamic movements of the system were modelled as planarly and it was used in walking movement. PID control was used to control the robot leg joints while walking. The performance of the target tracking and firing simulations was evaluated under the disruptive effects due to the walking motion. The elevation angle was calculated in order to track the objects whose coordinates were generated at random. It was observed that the robot tracked the targets at 3°, 6° and 9° with a maximum error of 0.6°. In addition, shootings were made to fixed targets located at 10 different coordinates. The largest shot error value was observed to be 16 cm. As a result, this research will make significant contributions to the defense industry.

Keywords: Fuzzy Control, Turret System, Four-Legged Robot, Barrel Stabilization, Shooting Simulation

Bulanık Mantık Kontrolü kullanarak hedeflere atış yapan dört bacaklı bir robotun dinamik simülasyonu

ÖZ

Bu çalışma, savunmada caydırıcılığı artırmak için engebeli arazi ve farklı çevre koşullarında dört bacaklı bir robot üzerine monte edilmiş silah ile hedefleri takip etmeyi ve vurmaya amaçlamaktadır. Sistemin dinamik hareketleri düzlemsel olarak modellenmiş ve yürüme hareketinde kullanılmıştır. Yürürken robot bacak eklemlerini kontrol etmek için PID kontrolü kullanılmıştır. Yürüme hareketi nedeniyle, bozucu etkiler altında hedef takip ve atış simülasyonlarının başarısı incelenmiştir. Koordinatları rastgele belirlenen hedeflerin takibi için namlu yükseklik açısı hesaplanmıştır. Robotun hedefleri maksimum 0,6° hata ile 3°, 6° ve 9°'de takip ettiği gözlemlenmiştir. Ayrıca 10 farklı koordinatta bulunan sabit hedeflere atışlar yapılmıştır. Maksimum atış hatası değerinin 16 cm olduğu görülmüştür. Dolayısıyla bu çalışma savunma sanayisine önemli katkılar sağlayacaktır.

Anahtar Kelimeler: Bulanık Kontrol, Taret Sistemi, Dört Bacaklı Robot, Namlu Stabilizasyonu, Atış Simülasyonu

I. INTRODUCTION

In recent years, robotic systems have emerged in all technological areas which mankind benefit from. Robotic systems and products are also widely used in the defense industry [1,2]. Especially multi-legged robots are preferred for their performance in rough terrain conditions. Multi-legged robots offer extra mobility compared to wheeled and other types of robots on uneven floors using foot soles used for each leg [3,4]. Compared to tracked and wheeled robots, legged robots perform better on rough terrain. [5]. In studies on legged robots, mostly four-legged robot studies [6-8] are encountered. Because, the speed-balance coordination of four-legged robots is more successful than robots with 6 or more legs. Quadruped robots have important advantages while walking on rough surfaces [9].

Usage of technological weapon systems in the defense field is increasing day by day. As gun systems gain the ability to work outside of human control depending on the advancement of technology, the importance attached to automatic gun systems increases day by day under the law [10]. Gun target assignment is a problem that aims to increase the hit rate. It is an important expectation that the gun system can make a successful hit under disruptive effects [11]. Successful hits from moving vehicles can be achieved by barrel stabilization. The design and implementation of an active stabilization system for gun systems can also reduce the physiological effects stemming from soldiers' war stress [12]. Studies on barrel stabilization [13,14], fire control systems [15,16], target tracking [17,18] can be found in the literature. Studies have been carried out in this area by using different control methods for weapon stabilization [19-21].

Many studies about robotics, were controlled by a fuzzy logic method in recent years. In the literature, there are many studies in which the fuzzy logic method for motion and trajectory control of mobile and anthropoid robots, air and land autonomous robots and manipulators are used [22-32]. The idea of fuzzy logic was discovered and suggested by L. A. Zadeh at the University of California, Berkeley in 1962 [33]. This discovery was considered valid when E. H. Mamdani at the University of London realized control applications with fuzzy logic [34]. In addition, studies on target tracking with fuzzy logic controller [35-37] have been done. There are also studies [38,39] in which walking motion using PID control method in quadruped robots.

In this study, a uniaxial gun system was located on a quadruped robot's body. To determine the dynamic behavior of the robot, the system was planarly modeled and simulated. Joints are controlled by PID method for balanced walking motion of the robot.

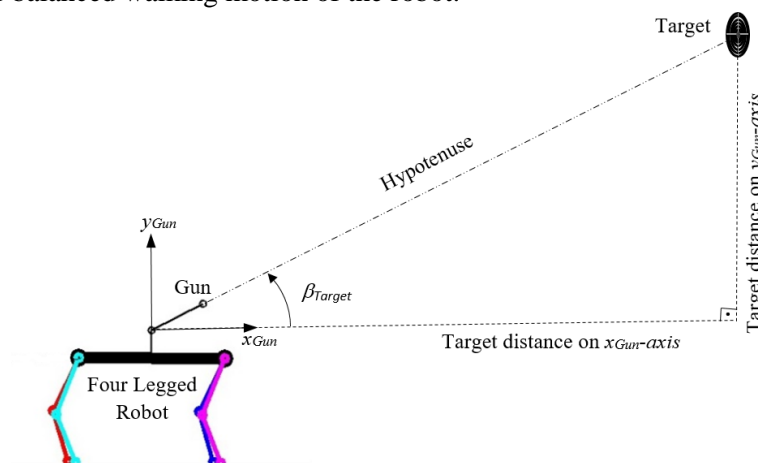


Figure 1. Shooting simulations of the four-legged robot towards the fixed target

To ensure that the gun follows the target accurately and fires toward fixed objects while the robot was moving, gun barrel stabilization was created. Due to the movement of the robot, the robot body causes

disruptive effects on the barrel system during the shooting at the fixed target. To keep the barrel in the reference coordinates against these disruptive effects, the Fuzzy Logic control method is used. An image of the shot made towards fixed targets is given in Figure 1. In the simulations, mathematical equations expressing the planar dynamic behavior of the projectile were used.

β_{target} calculation is made by using the hypotenuse value of the right triangle in the Pythagorean theorem, depending on the position error of the gun barrel in the horizontal and vertical axes with respect to the target. In the simulation, the robot's position relative to the fixed target constantly changes as the robot is walking. Therefore, since the barrel reference angle β_{target} will constantly change, this angle value needs to be updated for each position.

The study's entire content is explained in detail in the chapters denoted by their titles. The first chapter provides a theoretical overview of the significance of legged robots, automatic weapon control, four-legged robots, target identification and fire control systems, the necessity of barrel stability for successful shooting, and upcoming robot technologies. The kinematic study of the robot system was performed in the second chapter. Planar modeling was used in the third chapter to produce the system's dynamic behavior. The dynamic expressions of the system were then computed. The fourth chapter provides details on the PID control system used and the robot's "trot" walking simulation. Graphs of position and velocity were obtained as a result of the simulation. The control strategy based on fuzzy logic that was utilized to stabilize the barrel and effectively track the target is described in the following chapter. To offer barrel orientation to three different reference positions, control applications were simulated. This chapter contains the graphic results of the simulation of the system subjected to disruptive effects. In the sixth chapter, shooting simulations were created with many fixed targets that were distributed at random. These hits produced results that were shown in a table. The success rates of hits under particular physical conditions were looked at in the previous chapter. On the system, the impacts of the fuzzy logic control mechanism are discussed.

II. FORWARD AND INVERSE KINEMATIC ANALYSIS

Kinematic analysis in robotic systems is divided into two as forward and inverse kinematics. Forward kinematic is the determination of the end-effector configuration (position and orientation) of the robot for a given joint angle. Also, finding the necessary angles for the robot end-effector with a given position and orientation is known as inverse kinematics [40].

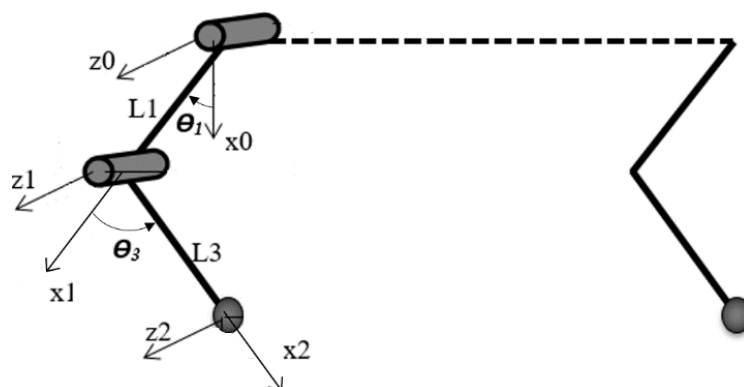


Figure 2. Axial placement of the robot's one leg

Denavit-Hartenberg method [41] was used to perform forward kinematic analysis. The D-H table created using this method was presented in Table 1. In addition, the axis set distribution of the single leg of the planar robot's single leg was given in Figure 2.

Table 1. D-H Table

| Link | θ | d | α | a |
|------|------------|-----|----------|-------|
| 1 | θ_1 | 0 | 0 | l_1 |
| 2 | θ_3 | 0 | 0 | l_3 |

The transformation matrices of the joints (A_i) are calculated by the obtained D-H table. The transformation matrix of the shoulder joint's end-effector on the robot leg was obtained as in (1) and (2). As a result, forward kinematic expressions were found with the expression in (3).

$${}^2_0T = A_1 A_2 \quad (1)$$

$${}^2_0T = \begin{bmatrix} \cos(\theta_1 + \theta_3) & -\sin(\theta_1 + \theta_3) & 0 & l_1 \cos \theta_1 + l_3 \cos(\theta_1 + \theta_3) \\ \sin(\theta_1 + \theta_3) & \cos(\theta_1 + \theta_3) & 0 & l_1 \sin \theta_1 + l_3 \sin(\theta_1 + \theta_3) \\ 0 & 0 & 1 & 0 \\ 0 & 0 & 0 & 1 \end{bmatrix} \quad (2)$$

$$\mathbf{p}_x = l_1 \cos \theta_1 + l_3 \cos(\theta_1 + \theta_3), \mathbf{p}_y = l_1 \sin \theta_1 + l_3 \sin(\theta_1 + \theta_3), \mathbf{p}_z = 0 \quad (3)$$

The inverse kinematic expressions of the robot's one leg were also given by using the forward kinematic equations obtained in (4) and (5).

$$\cos \theta_3 = \frac{\sqrt{p_x^2 + p_y^2 - l_1^2 - l_3^2}}{2l_1 l_3}, \sin \theta_3 = \pm \sqrt{1 - \cos^2 \theta_3}, \theta_3 = \arctan\left(\frac{\sin \theta_3}{\cos \theta_3}\right) \quad (4)$$

$$\cos \theta_1 = \frac{p_x l_3 \cos \theta_3 + p_y l_3 \sin \theta_3}{p_x^2 + p_y^2}, \sin \theta_1 = \pm \sqrt{1 - \cos^2 \theta_1}, \theta_1 = \arctan\left(\frac{\sin \theta_1}{\cos \theta_1}\right) \quad (5)$$

III. DYNAMIC ANALYSIS

The motion equations of the system were obtained to determine the dynamic behavior of a four-legged robot modeled as planarly. Robot's physical model was shown in Figure 3. When creating the physical model, it is assumed that all the joints of the robot have circular motion. The robot has four legs each with two degrees of freedom (2DOF). In addition, the robot body has a total of 3 degrees of freedom: a circular motion relative to the ground, a translational movement on the vertical axis and a translational movement on the horizontal axis. Finally, the gun system placed on the robot also has a single rotating joint. Thus, the system has 12 DOF totally. The parameter, expressed as "a" on the physical model, refers to the distance of the barrel system placed on the robot to body's center. Also, "b" is the barrel length and α represents the amount of angular rotation of the robot body relative to the ground. Using the physical model given in Fig. 1, the dynamic expressions were obtained according to the Lagrange-Euler method.

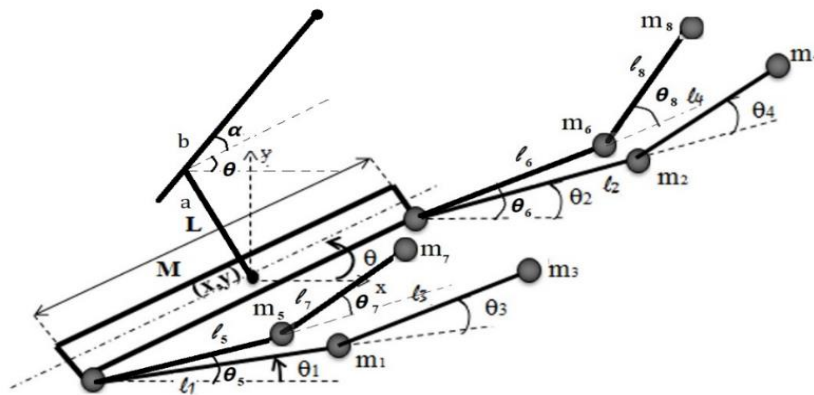


Figure 3. Quadruped robot's physical model

Schilling [42] argues that the use of the Lagrange-Euler method would be more efficient in achieving the result when creating a dynamic model of any robot mechanism. It is obtained by taking the difference of kinetic(T) and potential(V) energy in (6).

$$\frac{d}{dt} \frac{\partial}{\partial \dot{q}_i} L(q, \dot{q}_i) - \frac{\partial}{\partial q_i} L(q, \dot{q}_i) = \tau_i \quad 1 \leq i \leq n \quad (6)$$

Here, n represents the DOF number, q_i is the position of the moving components(legs or gun) in the system, i is the component index.

$$L = T - V \quad (7)$$

$$T = \frac{1}{2}M(\dot{x}^2 + \dot{y}^2) + \frac{1}{2}I\dot{\theta}^2 + \frac{1}{2}m_1(\dot{x}_1^2 + \dot{y}_1^2) + \frac{1}{2}m_2(\dot{x}_2^2 + \dot{y}_2^2) + \frac{1}{2}m_3(\dot{x}_3^2 + \dot{y}_3^2) + \frac{1}{2}m_4(\dot{x}_4^2 + \dot{y}_4^2) + \frac{1}{2}m_5(\dot{x}_5^2 + \dot{y}_5^2) + \frac{1}{2}m_6(\dot{x}_6^2 + \dot{y}_6^2) + \frac{1}{2}m_7(\dot{x}_7^2 + \dot{y}_7^2) + \frac{1}{2}m_8(\dot{x}_8^2 + \dot{y}_8^2) + \frac{1}{2}m_n(\dot{x}_n^2 + \dot{y}_n^2) \quad (8)$$

$$V = Mgy + m_1gy_1 + m_2gy_2 + m_3gy_3 + m_4gy_4 + m_5gy_5 + m_6gy_6 + m_7gy_7 + m_8gy_8 + m_ngy_n \quad (9)$$

System's Lagrange expression was found with (7), where the total kinetic energy of the system was found with (8) and the total potential energy of the system was found with (9). The explanations of the physical parameters in the equations were given in Nomenclature.

In order to obtain the kinetic and potential energy expressions, the position equations of the robot body and legs must be determined as in Appendix-1. Velocity equations were calculated as a result of time-based derivatives of position expressions of all joints. The Lagrange equation was derived from velocity expressions as in Appendix-2. When the Lagrange equation was adapted according to (6), the dynamic motion equations will be found to calculate the appropriate torque values required by all joints on the system. The mathematical expressions of the dynamic motion equations were also included in Appendix-3. The Jacobian matrix form generated in (10) should be used to transmit the reaction force of the ground to the robot body during the movement of the robot and to determine the effects of this force.

$$[J] = \begin{bmatrix} \frac{\partial x_i}{\partial x} & \frac{\partial x_i}{\partial y} & \frac{\partial x_i}{\partial \theta} & \frac{\partial x_i}{\partial \theta_1} & \frac{\partial x_i}{\partial \theta_2} & \frac{\partial x_i}{\partial \theta_3} & \frac{\partial x_i}{\partial \theta_4} & \frac{\partial x_i}{\partial \theta_5} & \frac{\partial x_i}{\partial \theta_6} & \frac{\partial x_i}{\partial \theta_7} & \frac{\partial x_i}{\partial \theta_8} \\ \frac{\partial y_i}{\partial x} & \frac{\partial y_i}{\partial y} & \frac{\partial y_i}{\partial \theta} & \frac{\partial y_i}{\partial \theta_1} & \frac{\partial y_i}{\partial \theta_2} & \frac{\partial y_i}{\partial \theta_3} & \frac{\partial y_i}{\partial \theta_4} & \frac{\partial y_i}{\partial \theta_5} & \frac{\partial y_i}{\partial \theta_6} & \frac{\partial y_i}{\partial \theta_7} & \frac{\partial y_i}{\partial \theta_8} \end{bmatrix} \quad (10)$$

$$[J] = \begin{bmatrix} \frac{\partial x_n}{\partial x} & \frac{\partial x_n}{\partial y} & \frac{\partial x_n}{\partial \theta} & \frac{\partial x_n}{\partial \theta_1} & \frac{\partial x_n}{\partial \theta_2} & \frac{\partial x_n}{\partial \theta_3} & \frac{\partial x_n}{\partial \theta_4} & \frac{\partial x_n}{\partial \theta_5} & \frac{\partial x_n}{\partial \theta_6} & \frac{\partial x_n}{\partial \theta_7} & \frac{\partial x_n}{\partial \theta_8} & \frac{\partial x_n}{\partial \alpha} \\ \frac{\partial y_n}{\partial x} & \frac{\partial y_n}{\partial y} & \frac{\partial y_n}{\partial \theta} & \frac{\partial y_n}{\partial \theta_1} & \frac{\partial y_n}{\partial \theta_2} & \frac{\partial y_n}{\partial \theta_3} & \frac{\partial y_n}{\partial \theta_4} & \frac{\partial y_n}{\partial \theta_5} & \frac{\partial y_n}{\partial \theta_6} & \frac{\partial y_n}{\partial \theta_7} & \frac{\partial y_n}{\partial \theta_8} & \frac{\partial y_n}{\partial \alpha} \end{bmatrix} \quad (11)$$

When the appropriate parameters were adapted to this Jacobian matrix form, the expressions showing the effect of the movements on the horizontal and vertical axes to the body and legs were shown in Appendix-4. The Jacobian matrix form, which calculates the effect of movements of the gun barrel with a single degree of freedom on the body was given in (11), and the gun barrel Jacobian was also given in Appendix 5. The numerical values of the four-legged robot's physical parameters with the gun barrel system were given in Table 2.

Table 2. Physical Parameters of the Robot

| Parameter | Value | Parameter | Value |
|----------------------|--------|----------------------|--------|
| M | 12 kg | m_1, m_2, m_5, m_6 | 1.5 kg |
| l_g | 0.8 m | m_3, m_4, m_7, m_8 | 0.5 kg |
| l_1, l_2, l_5, l_6 | 0.24 m | a | 0.1 m |
| l_3, l_4, l_7, l_8 | 0.2 m | b | 0.3 m |
| m_n | 0.6 kg | | |

IV. WALKING PATTERN AND SIMULATION WITH PID CONTROL OF FOUR-LEGGED ROBOT

The traditional PID controller for automated systems is widely used in industry. This is because the PID controllers are easy to understand and implement [43]. In PID method, the control signal is obtained as in (12) according to the proportional (P), integral (I) and derivative (D) coefficients.

$$u(t) = K_p e(t) + K_d \frac{d e(t)}{d t} + K_i \int_0^t e(t) d t \quad (12)$$

K_p in equation (12) refers to the proportional coefficient, K_d refers to the derivative coefficient and K_i is the integral coefficient. The integral term gives a control output that is proportional to the time integral of the error. This ensures that the permanent status error is zero [44]. The controller's P, I and D coefficients were chosen as $K_p=500$, $K_d=50$, $K_i=0.1$ by trial-and-error technique.

Trajectory planning of the robot is done by determining the angular reference positions that the robot's legs need to track. PID controller was applied to the system to bring these joints into reference angles. Four-legged robots have four different types of gaits, such as "walking, pacing, trotting, galloping". The most commonly used mode of movement is the "trotting" gait. Because with this gait, the movement of the robot can be achieved at any desired velocity in a limited range [45]. The trot gait pattern shown in Fig. 4. was used for simulations [46]. Due to difficulty in walking control, many four-legged robot studies were performed using a "trot" gait, in which a front leg and a rear leg move in pairs [47]. The motion of this gait pattern has a disruptive effect on the barrel stabilization.



LF: Left Forward Leg, **RF:** Right Forward Leg, **LB:** Left Back Leg, **RB:** Right Back Leg

Figure 4. Trot gait pattern of quadruped robots

Figure 5 shows that the robot's foot follows a sinusoidal path in the horizontal and vertical axis while one leg steps during the trot walk. The leg has two phases, in the air (flight) and the ground (stance). The robot is in the stance phase when it is in touch with the ground. When contact with the ground is lost, the flight phase begins.

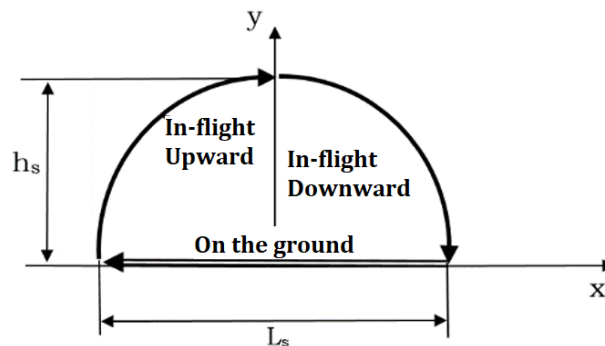


Figure 5. Robot leg's one step trajectory

The sinus function that calculates the trajectory that the robot leg should follow in flight phase was given in (13). h_{step} is leg's height from the ground. The ω is the step movement's frequency. L_s

indicates the amount of translation of the leg at x-direction in one step. If the walking time for a period is shown in T_G , the V_r translation velocity can be calculated as shown in (14).

$$h_s = h_{step} \sin(2\pi\omega t) \quad (13)$$

$$V_r = \frac{L_s}{T_G} \quad (14)$$

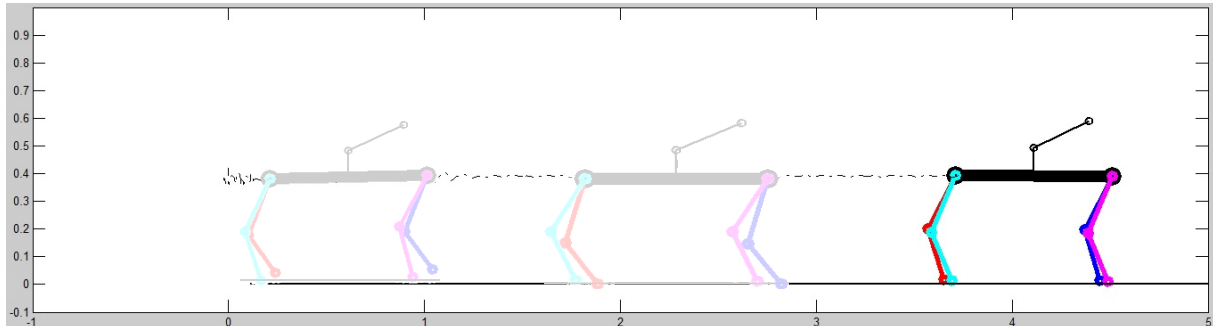


Figure 6. *Four legged robot's trot gait simulation*

Quadruped robot's trot gait was simulated. As shown in the simulation image in Fig. 6., the robot appears to have advanced about 4 meters. The walking motion is a 7-second simulation and results were given graphically in Fig. 7. According to the graphs, in the first moments of the walking, body center's up-and-down oscillation amplitude on the vertical axis is observed to be around 0.05 m. Similarly, the body's angular swing was around 2° - 3° . These amplitudes have decreased considerably as of the third second of the simulation. In addition, the robot continues to move horizontally with 1 m / s velocity.

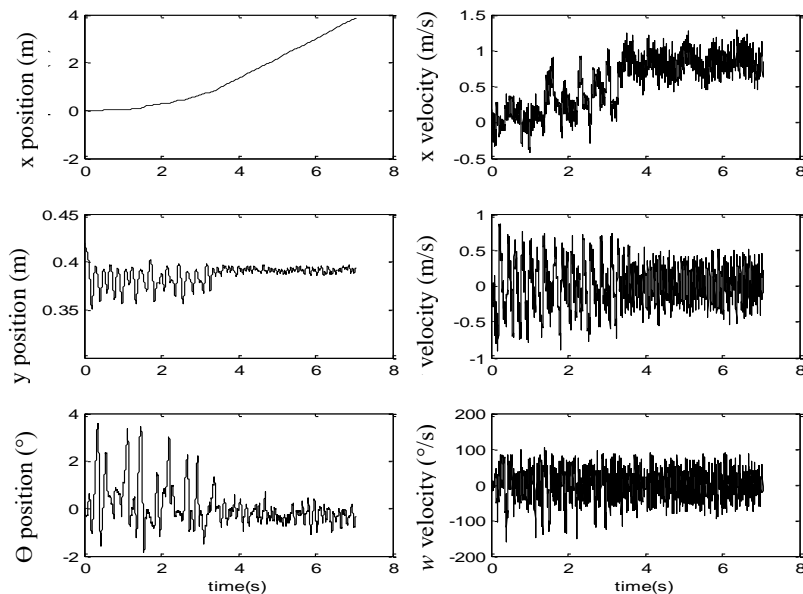


Figure 7. *Quadruped robot's position and velocity graphs*

V. APPLICATION OF THE GUN BARREL STABILIZATION FOR A QUADRUPED ROBOT DURING WALKING WITH FUZZY LOGIC CONTROL METHOD

The main point on which fuzzy logic controllers are based is the incorporation of an expert system operator's knowledge, experience, intuition, and control strategy as a knowledge base in the controller's design. Verbal rules based on knowledge and experience are used to carry out control

procedures. For example, if an expert identifies the control behaviors necessary for the system in verbal terms such as "small", "fast", and "slow", the rules to be created with "IF-THEN" commands will be obtained by using verbal terms [48].

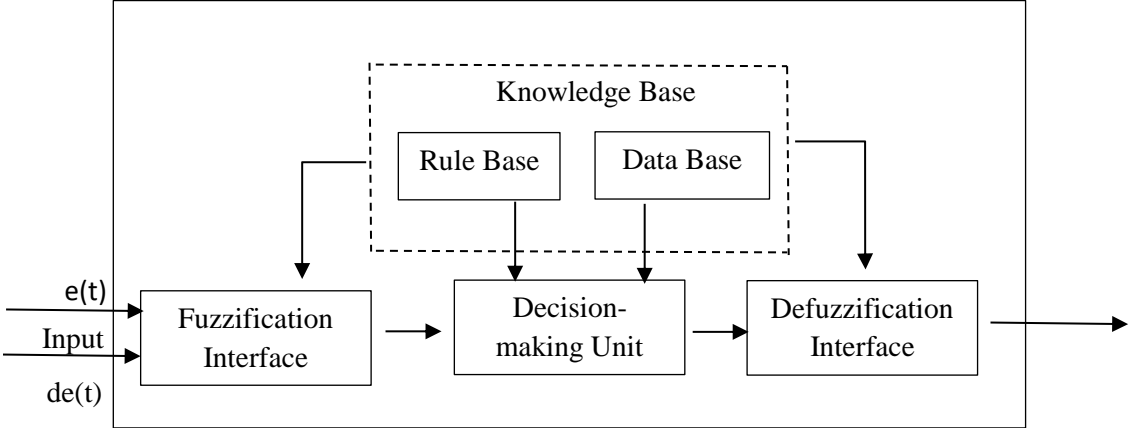


Figure 8. The basic structure of a fuzzy logic control system

Basic structure of the Fuzzy Logic control system is given in Fig. 8. [49]. Fuzzy Control System consists of four basic units. The concept of fuzzy logic functions like the human sense and inference mechanism. Fuzzy logic, unlike other classical control methods, performs the inspection by taking the intermediate values between two values into account. The output of the fuzzy controller consists of blurring input and output values using the associated membership functions. The input value has a different meaning through the associated membership function.

Fuzzy logic control method was used for gun barrel stabilization. The control signal was calculated at the output by considering the error and the derivative-error at the fuzzy logic control input. Triangular membership functions were used in the fuzzy logic control structure. The boundary values of the membership functions were determined by trial and error techniques. The rule table for input and output was shown in Table 3.

Table 3. Rule table for membership functions

| | | Derivative of the Error (d _e /d _t) | | |
|-----------|----|---|-----|-----|
| | | dNe | dZe | dPe |
| Error (e) | Ne | Nu | Zu | Nu |
| | Ze | Nu | Zu | Pu |
| | Pe | Pu | Zu | Pu |

The membership functions specified for the error input are given in Fig. 9. Definitions of the expressions in Table 3 are given below;

- Ne:** Negative Error, **dNe:** Derivative Negative Error
- Ze:** Zero Error, **dZe:** Derivative Zero Error
- Pe:** Positive Error, **dPe:** Derivative Positive Error
- Nu:** Negative Control Output
- Zu:** Zero Control Output
- Pu:** Positive Control Output

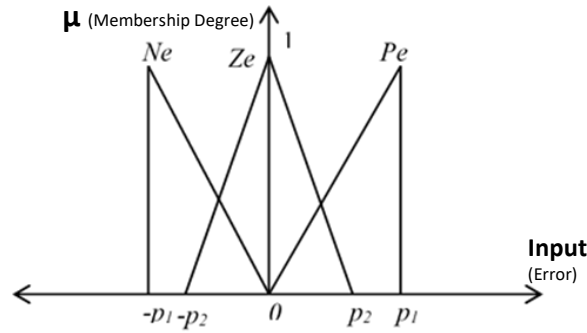


Figure 9. Membership functions for error input (e)

The determined membership functions of the input which is the derivative of the error are given in Fig. 10. The membership functions of the control output are given in Fig. 11.

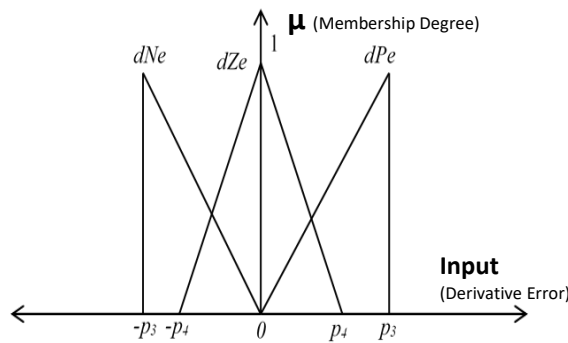


Figure 10. Membership functions for derivative error input (d_e/d_t)

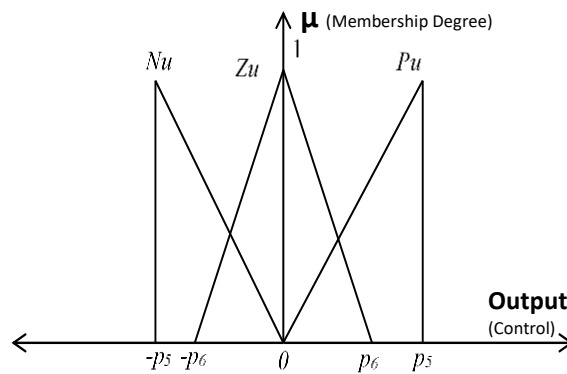


Figure 11. Membership functions for control output (u)

The limit values of the membership functions in the fuzzy logic control structure were determined as the numerical values shown in Table 4. by trial and error technique.

Table 4. Limit values for membership functions

| p_1 | p_2 | p_3 | p_4 | p_5 | p_6 |
|-------|-------|-------|-------|-------|-------|
| 10 | 1 | 100 | 10 | 50 | 10 |

Shooting simulations were performed at three different reference target angles 3° , 6° , and 9° during the walking movement. These target angles were randomly determined considering the difficulty of tracking targets at very narrow angles. It has been shown that by choosing small values as in the

reference angles, the robot tracks the target more precisely under the disruptive effects and makes successful hits on the target. Controls were made for three different target angles during walking. The initial barrel angle is accepted as zero in simulations. As mentioned earlier, the barrel reference angle is equal to the sum of the relative angle of the barrel and the relative angle of the ($\beta_{target}=\alpha+\theta$).

Target-1;

The system responses of the simulation trying to keep the β_{target} angle at 3° relative to the ground are presented in Figure 12. Gun barrel's angular position relative to the body α is oscillating in relation to body motions. The controller followed the target by instantly calculating the β_{target} reference angle with very small errors and oscillations. This error was found to be 0.57° maximum.

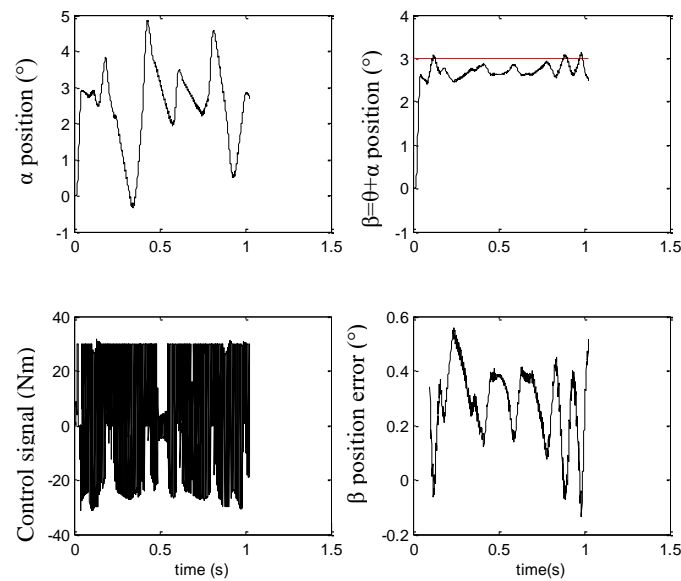


Figure 12. System responses for $\beta_{target}=3^\circ$ in simulation

Target-2;

The system responses of the simulation performed while trying to keep the β_{target} angle at 6° relative to the ground, were presented graphically in Fig. 13. The angular position error value is about 0.62° .

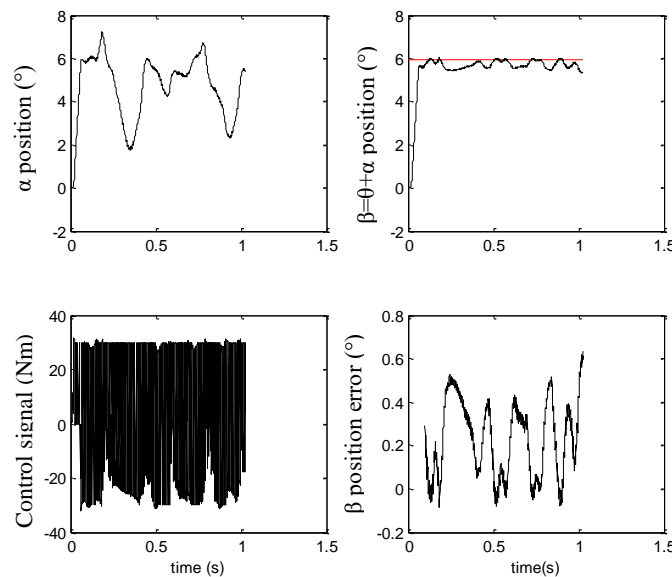


Figure 13. System responses for $\beta_{target}=6^\circ$

Target-3;

The system responses of the simulation performed while trying to keep the β_{target} angle at 9° relative to the ground, are showed in Fig. 14. The angular error size around the reference position is no more than 0.6° . Shooting was made at $t = 1s$ of the simulations. Therefore, the graphics show the part where the gun tracks the target until the shooting was made. It is evident from the presented graphs that the Fuzzy Logic controller used in the simulations can hold the barrel around the reference position very successfully.

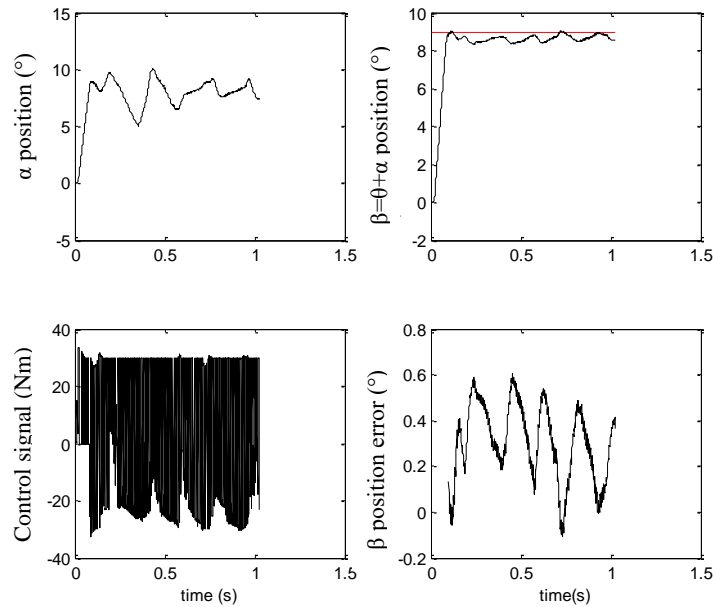


Figure 14. System responses for $\beta_{target} = 9^\circ$

VI. SHOOTING SIMULATIONS

The success of shooting simulations to fixed targets with random coordinates was evaluated. Hits were made with disruptive effects while the robot was walking. In simulations, the dynamic equations of the bullet used to hit the target were also taken into account. Figure 15 is the block diagram expressing the control loop of the system.

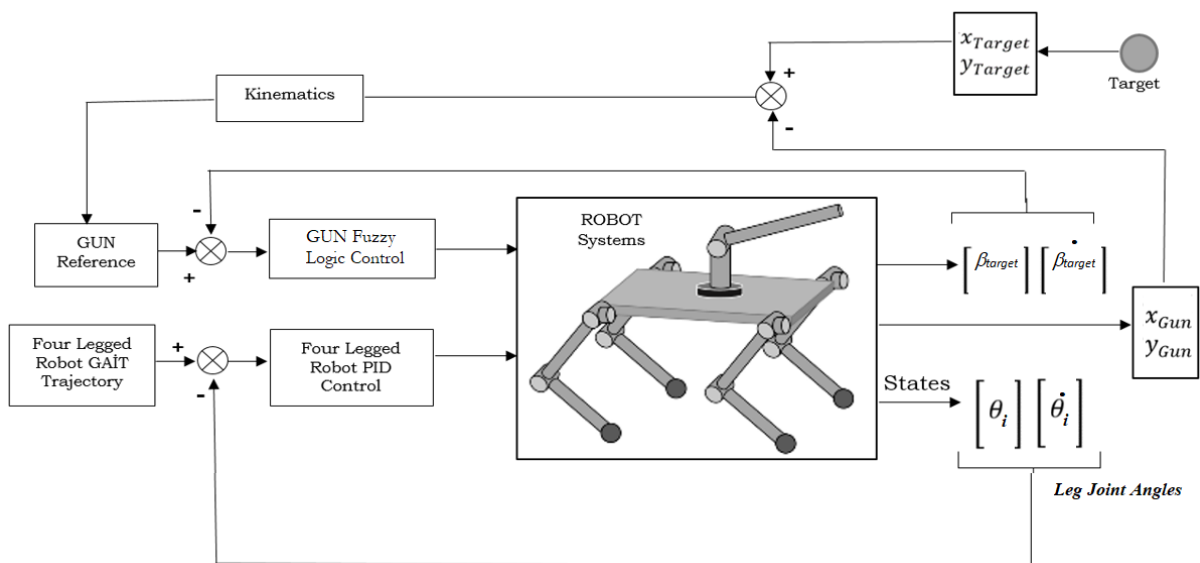


Figure 15. Control loop diagram of the system

In the dynamics of the projectile, environmental conditions, penetration pressure at the moment of impact and projectile's physical parameters were used. Related to this, the graph in Figure 16 taken from study [50] shows the change in bore pressure and velocity of the projectile depending on the length of the barrel. Bullet ballistic curves in the barrel were used.

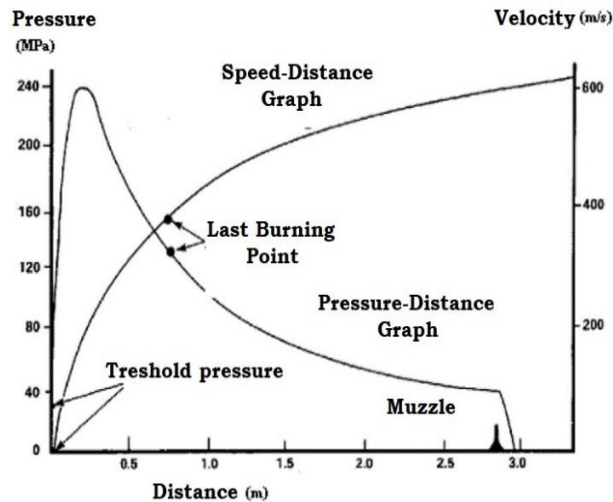


Figure 16. Features in gun barrel

Looking at the Fig. 16, the pressure steadily rises to the maximum. Depending on the barrel length, the pressure value starts to decrease again till the bullet leaves the barrel. The time it takes for bullets to exit the barrel is as short as 5-10 milliseconds, depending on the rate of combustion.

Table 5. Projectile features

| Technical Characteristics | | | |
|-------------------------------------|------------------------|---------------------------------|--------------------------|
| <u>Specification</u> | Stanag 4090 | <u>Projectile Contact Force</u> | min. 20,4 kgf |
| | | <u>Shell Model Number</u> | 9 mmx19 parabellum shell |
| <u>Cartridge Length</u> | 29,69 – 0,3 mm | <u>Projectile Weight</u> | 8 ±0,075 g |
| <u>Cartridge Weigth</u> | ~12,15 g | <u>Shell Material</u> | Brass (CuZn30) |
| <u>Velocity</u> | 370 ± 10 m/s (in 16 m) | <u>Capsule</u> | 9 mm capsule, boxer |
| <u>Velocity Standart Deviation</u> | max. 9 m/s | | |
| <u>Average shell mouth pressure</u> | max. 2850 bar | | |
| <u>Distribution</u> | max. 7,6 cm (in 46 m) | | |

Technical properties of 9 mm parabellum bullet were used. These technical specifications were given in Table 5. [51]. Projectile core other than shell weighs $m_{projectile} = 8$ grams. The physical model was shown in Fig. 17. indicates the dynamic behavior of the projectile during the planar movement.

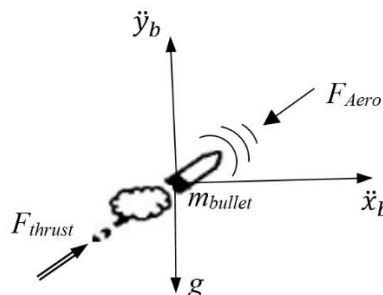


Figure 17. The physical model of the projectile

The projectile core, which is accepted as the point mass, can move linearly along the x-axis and y-axis. The projectile fired from the gun barrel with F_{thrust} force leaves the barrel with V_b velocity. From this moment on, only the gravity and the F_{Aero} frictional force caused by the atmosphere influence the projectile core during its aerial movement. The thrust pressure P_b was calculated as in (15).

The parameters in the model $P=1500$, $\lambda=500$, $\omega_b=50$ are defined numerically. It was presumed that the time t for projectiles leaving the barrel is within the range of (0-10) milliseconds. Since the shooting was made at $t = 1$ s, the thrust force and velocity remained constant from that moment on. F_{thrust} is calculated as in (16). A_b refers to the surface area under pressure.

$$P_b = P e^{-\lambda t} \sin(2\pi\omega_b t) \quad (15)$$

$$F_{thrust} = A_b P_b \quad (16)$$

Planar dynamics analysis of the bullet was carried out according to Newton's laws of motion. x_b is the equations on the horizontal axis and y_b on the vertical axis. Also, g is the acceleration of gravity. The friction force F_{Aero} , which occurs while moving with V_b velocity in the atmosphere, is calculated by (19).

$$\ddot{x}_b = \frac{F_{thrust}^x - F_{Aero}^x}{m_{bullet}} \quad (17)$$

$$\ddot{y}_b = \frac{F_{thrust}^y - F_{Aero}^y - g}{m_{bullet}} \quad (18)$$

$$F_{Aero} = \frac{1}{2} \rho S C_d V_b^2 \quad (19)$$

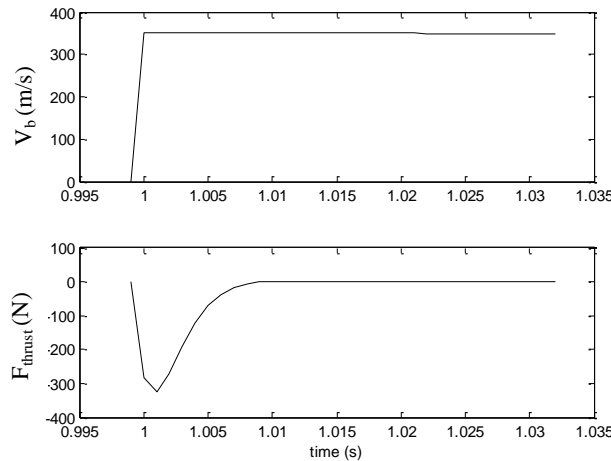


Figure 18. Ballistics of projectile

ρ is the density of air, S is the surface area perpendicular to the bullet's direction of advance. Friction coefficient between the projectile and the air was $C_d=0.12$. The temporal change of F_{thrust} and V_b during shooting simulation is given in Figure 18. The coordinates of the fixed targets were determined randomly, ranging from 5-12 meters horizontally and 0.5-2 meters vertically. During this one-second period, the barrel stabilization, which is necessary to point the gun at the target, is provided by the fuzzy logic control method. β_{target} was calculated instantaneously, considering the robot's variable position during walking. The reference angle can be calculated by the expression (20), depending on the e_x -gun position error in horizontal axis and the e_y in vertical axis.

$$\beta_{target} = \text{atan2} \left(\frac{e_y}{e_x} \right) = \text{atan2} \left(\frac{y_{target} - y_{gun}}{x_{target} - x_{gun}} \right) \quad (20)$$

System was simulated with the Runge-Kutta method. This method is frequently used in numerical solutions of differential equations [52]. Fig. 19. shows the simulation image of a precise hit made by the four-legged robot while walking.

Table 6. Shooting control results of projectile

| Target Number | x_{target} (m) | y_{target} (m) | Error (m) |
|---------------|------------------|------------------|-----------|
| 1 | 14.18 | 1.27 | 0.16 |
| 2 | 12.64 | 0.79 | 0.07 |
| 3 | 8.93 | 1.88 | 0.13 |
| 4 | 12.56 | 1.94 | 0.06 |
| 5 | 9.09 | 1.13 | 0.05 |
| 6 | 6.63 | 1.28 | 0.05 |
| 7 | 7.51 | 0.66 | 0.14 |
| 8 | 13.12 | 1.90 | 0.10 |
| 9 | 11.22 | 0.65 | 0.07 |
| 10 | 9.16 | 1.50 | 0.16 |

According to Table 6 target coordinate and error values for 10 different fixed targets were given in Table 6. The highest product error value is found as 0.16 m in the 1st and 10th throws. The smallest product error value was 0.05 m. Mean value is 0.099 m and the standard deviation is calculated as 0.044 m.

The main purpose of this study is to keep the barrel at the target in the face of disruptive effects. Fuzzy Logic control method has been applied and the success of this controller on target hit has been studied. Looking at Table 6, it is evident that fixed targets are chosen randomly between 5 and 15 meters in the horizontal axis and between 0.5 and 1.5 meters in the vertical axis. In order to see the stabilization success, it was required to shoot at short distance targets in the horizontal direction. Because, if the distance to the horizontal target is increased, the bullet reaches the target with a greater deviation due to gravity.

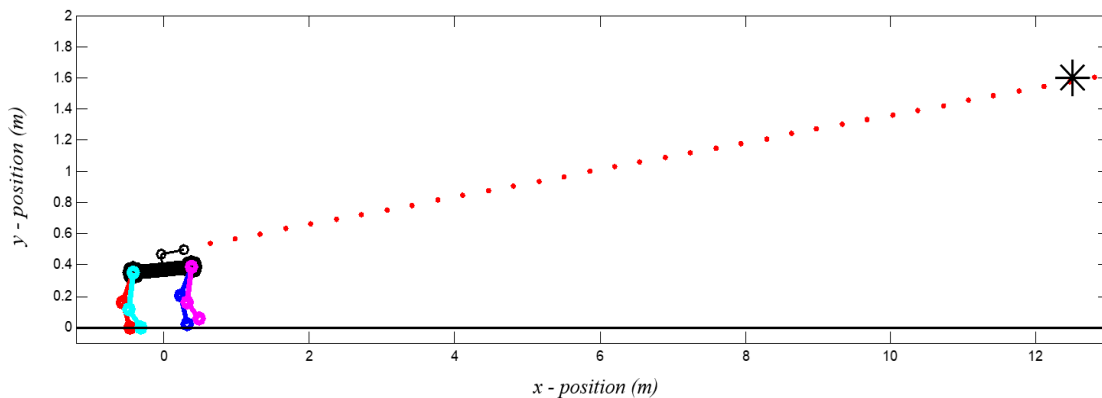


Figure 19. Shooting control simulation of projectile

VII. RESULTS AND RECOMMENDATIONS

In this work, a DOF-equipped gun turret was mounted on a four-legged robot. The main objective is to guide the gun toward the target, track the target, and assure accurate striking while stabilizing the gun barrel while the robot is moving. A planar model of the system was used. Considering that walking and shooting simulations require a planar model. Additionally, it serves as the foundation for experiments. Trot walking patterns were used to simulate movement. The robot body's oscillation during this walking was perceived as having a disruptive effect on the gun turret. The barrel was pointed at the target using a fuzzy logic control mechanism under this disruptive impact. Trial and error technique was used to determine the controller's parameters. According to the results, the maximum product error value in shooting towards fixed targets from a four-legged robot was 0.16 m.

The results can be compared, and strategies to improve the success rate can be devised, by using a variety of control methods with diverse characteristics with the research to be done in this subject.

Nomenclature

| | | | |
|----------------|---|------------------|---|
| M | Robot Body(RB)'s mass | β_{target} | Barrel reference angle |
| x | RB's position in horizontal axis | m_n | Gun barrel(GB) mass |
| y | RB's position in vertical axis | w | Step motion's frequency |
| m_{1-8} | Leg limbs(LL)' masses | L_s | Step length |
| θ | RB's angular position to floor by vertical axis | F_{thrust} | Projectile force |
| θ_{1-8} | LL's angular positions | F_{aero} | Frictional force (atmosphere and gravity) |
| l_g | RB's length | V_b | Projectile velocity |
| l_{1-8} | LL's lengths | P_b | Repulsion pressure |
| a | Gun turret length | A_b | Pressure surface area |
| b | Gun barrel length | C_d | Friction coefficient between projectile and air |
| x_{1-8} | LL's positions in horizontal axis | x_{target} | Target position on the horizontal axis |
| y_{1-8} | LL's positions in vertical axis | y_{target} | Target position on the vertical axis |
| I | Body's moment of inertia | e_x | Horizontal position error |
| α | Gun barrel's relative angular position to body | e_y | Vertical position error |
| x_n | Gun barrel(GB) position on the horizontal axis | y_n | Gun barrel(GB) position on the vertical axis |

Funding: There isn't any funding source for this research.

Conflict of Interest: Ahmet Burak TATAR, Alper Kadir TANYILDIZI, Beyda TAŞAR and Oğuz YAKUT declare that they have no conflict of interest.

Data Availability Statement: All data used to support the findings of this study are included within the article.

Acknowledgement

This study was produced as part of the doctoral thesis titled "Four-Legged Hunter Robot" carried out under the supervision of Prof. Dr. Oğuz YAKUT in the Department of Mechatronics Engineering, Faculty of Engineering at Firat University.

ORCID

Ahmet Burak TATAR  <http://orcid.org/0000-0001-5848-443X>
 Alper Kadir TANYILDIZI  <http://orcid.org/0000-0003-3324-5445>
 Beyda TAŞAR  <http://orcid.org/0000-0002-2771-3524>
 Oğuz YAKUT  <http://orcid.org/0000-0002-0986-1435>

VIII. REFERENCES

- [1] S. Zhang, J. Yao, Y. Wang, Z. Liu, Y. Xu, Y. Zhao, "Design and motion analysis of reconfigurable wheel-legged mobile robot", *Defence Technology*, 18, 1023-1040, 2022 doi: 10.1016/j.dt.2021.04.013
- [2] K.L. Foster, M.D. Petty, "Estimating the tactical impact of robot swarms using a semi-automated forces system and design of experiments methods", *The Journal of Defense Modeling and Simulation*, 18(3), 247-269, 2021 doi: 10.1177/15485129211008532

- [3] J.T. Machado, M.F. Silva, “An overview of legged robots”, *International symposium on mathematical methods in Engineering. Çankaya, Ankara, Turkey*, 1-39 (2015).
- [4] J. Liu, M. Tan, X. Zhao, “Legged robots-an overview”, *Trans Inst. Meas. Control.* 29(2), 185-202, 2007 doi: 10.1177/0142331207075610
- [5] X. Ding, H. Chen, “Dynamic modelling and locomotion control for quadruped robots based on center of Inertia on SE(3)”, *Journal of Dynamic Systems, Measurement, and Control*, 138, 011004/1-8, 2016 doi: 10.1115/1.4031728
- [6] X. Chang, H. Ma, H. An, “Quadruped Robot Control through Model Predictive Control with PD Compensator”, *International Journal of Control, Automation and Systems*, 19(11), 3776-3784, 2021 doi: 10.1007/s12555-020-0734-9
- [7] Y. Zheng, K. Xu, Y. Tian, H. Deng, X. Ding, “Bionic Design and Analysis of a Novel Quadruped Robot with a Multistage Buffer System”, *Chinese Journal of Mechanical Engineering*, 35(32), 2-21, 2022 doi: 10.1186/s10033-022-00700-9
- [8] J. Cui, Z. Li, J. Qiu, T. Li, “Fault-tolerant motion planning and generation of quadruped robots synthesised by posture optimization and whole body control”, *Complex&Intelligent Systems*, 8, 2991-3003, 2022 doi: 10.1007/s40747-022-00652-6
- [9] M.U. Atique, R.I. Sarker, A.R. Ahad, “Development of an 8DOF quadruped robot and implementation of inverse kinematics using Denavit-Hartenberg convention”, *Heliyon* 01053, 1-19, 2018 doi: 10.1016/j.heliyon.2018.e01053
- [10] N. Weizmann, “Autonomous weapon system under international law”, *Academy Briefing.* 8, pp. 3, 2014.
- [11] M.A. Şahin, K. Leblebicioğlu, “Approximating the optimal mapping for weapon target assignment by fuzzy reasoning”, *Information Sciences* 255, 30-44, 2014 doi: 10.1016/j.ins.2013.08.004
- [12] A.P. White, “Control design for an inertially stabilized rifle”, *Master Thesis, Faculty of the Virginia Polytechnic Institute and State University, Department of Electrical Engineering, Blacksburg, Virginia*, pp. 1, 2007
- [13] W. Rone, P.B. Tzvi, “Dynamic modeling and simulation of a yaw-angle quadruped maneuvering with a planar robotic tail”, *Journal of Dynamic Systems Measurement and Control* 138, 084502/1-7, 2016 doi: 10.1115/1.4033103
- [14] Ö. Özüğür, M.K. Leblebicioğlu, “Shooter localization using sensor networks and optimization based fusion process”, *The Journal of Defense Sciences* 15, 207-235, 2016
- [15] J. Shukla, “Dynamic analysis of gun control system of main battle tank”, *International Journal of Heavy Vehicle Systems*, 28(2), 2022.
- [16] İ.S. Kuseyri, “Stabilization and DOB-Based Disturbance Rejection for MBT Gun-Barrel Elevation Drive”, *Int. J. Adv. Eng. Pure Sci.*, 32(2), 206-211, 2020.
- [17] M.F. Hocaoglu, “Weapon target assignment optimization for land based multi-air defense systems: A goal programming approach”, *Computers & Industrial Engineering* 128, 681-689, 2019 doi: 10.1016/j.cie.2019.01.015
- [18] I.B. Saksvik, A. Alcocer, V. Hassani, A. Pascoal, “Target Tracking of an Underwater Glider Using a Small Unmanned Surface Vessel”, *IFAC PapersOnLine*, 55(31), 478-483, 2022 doi: 10.1016/j.ifacol.2022.10.473
- [19] A.B. Tatar, A.K. Tanyıldızı, O. Yakut, “Four legged hunter (FLH) robot: design and shooting control to moving targets with SMC”, *Simulation Modelling Practice and Theory*, 104, 102117, 1-15, 2020.
- [20] A.B. Tatar, A.K. Tanyıldızı, O. Yakut, “Shooting control application from a quadruped robot with a weapon system via Sliding-mode Control method”, *Defence Science Journal*, 70(4), 404-411, 2020.
- [21] A.B. Tatar, B. Taşar, O. Yakut, “A shooting control application of four-legged robots with gun turret”, *Arabian Journal for Science and Engineering*, 45, 5191-5206, 2020.
- [22] O. Castillo, H. Neyoy, J. Soria, P. Melin, F. Valdez, “A new approach for dynamic fuzzy logic parameter tuning in Ant Colony Optimization and its application in fuzzy control of a mobile robot”, *Applied Soft Computing* 28, 150–159, 2015 doi: 10.1016/j.asoc.2014.12.002
- [23] F. Abdessemed, M. Faisal, M. Emmadeddine, R. Hedjar, K. Al-Mutib, M. Alsulaiman, H. Mathkour, “A Hierarchical Fuzzy Control Design for Indoor Mobile Robot”, *International*

- Journal of Advanced Robotic Systems* 11(33), 2014 doi: 10.5772/57434
- [24] E. Kayacan, H. Ramon, W. Saeys, “Adaptive Neuro-Fuzzy Control of a Spherical Rolling Robot Using Sliding-Mode-Control-Theory-Based Online Learning Algorithm”, *IEEE Transactions On Cybernetics* 43(1), 2013 doi: 10.1109/TSMCB.2012.2202900
- [25] I. Siradjuddin, L. Behera, T. M. McGinnity, “Image-Based Visual Servoing of a 7-DOF Robot Manipulator Using an Adaptive Distributed Fuzzy PD Controller”, *IEEE/ASME Transactions On Mechatronics* 19(2), 2014 doi: 10.1109/TMECH.2013.2245337
- [26] Q. Zhou, H. Li, P. Shi, “Decentralized Adaptive Fuzzy Tracking Control for Robot Finger Dynamics”, *IEEE Transactions On Fuzzy Systems* 23(3), 2015 doi: 10.1109/TFUZZ.2014.2315661
- [27] C.F. Juang, Y.H. Chen, Y.H. Jhan, “Wall-Following Control of a Hexapod Robot Using a Data-Driven Fuzzy Controller Learned Through Differential Evolution”, *IEEE Transactions On Industrial Electronics* 62(1), 2015 doi: 10.1109/TIE.2014.2319213
- [28] Z. Li, S. Xiao, S.S. Ge, H. Su, “Constrained Multilegged Robot System Modeling and Fuzzy Control With Uncertain Kinematics and Dynamics Incorporating Foot Force Optimization”, *IEEE Transactions On Systems, Man, And Cybernetics: Systems* 46(1), 2016 doi: 10.1109/TSMC.2015.2422267
- [29] H. Li, C. Wu, S. Yin, H.K. Lam, “Observer-Based Fuzzy Control for Nonlinear Networked Systems Under Unmeasurable Premise Variables”, *IEEE Transactions On Fuzzy Systems* 24(5), 2016 doi: 10.1109/TFUZZ.2015.2505331
- [30] Y. Takahashi, T. Ishii, C. Todoroki, Y.I. Maeda, T. Nakamura, “Fuzzy Control for a Kite-Based Tethered Flying Robot”, *Journal of Advanced Computational Intelligence and Intelligent Informatics* 19(3), 2015 doi: 10.1109/FUZZ-IEEE.2014.6891839
- [31] M.A. Sanchez, O. Castillo, J. R. Castro, “Generalized Type-2 Fuzzy Systems for controlling a mobile robot and a performance comparison with Interval Type-2 and Type-1 Fuzzy Systems”, *Expert Systems with Applications* 42, 5904–5914, 2015 doi: 10.1016/j.eswa.2015.03.024
- [32] P. Melin, L. Astudillo, O. Castillo, F. Valdez, M. Garcia, “Optimal design of type2 and type-1 fuzzy tracking controllers for autonomous mobile robots under perturbed torques using a new chemical optimization paradigm”, *Expert Systems with Applications* 40, 3185–3195, 2013 doi: 10.1016/j.eswa.2012.12.032
- [33] L. A. Zadeh, “Fuzzy Sets”, *Information and Control* 8, 338-353, 1965
- [34] E.H. Mamdani, S. Assilian, “An Experiment in Linguistic Synthesis With a Fuzzy Logic Controller”, *International Journal of Man-Machine Studies* 7, 1-13, 1974 doi: doi.org/10.1006/ijhc.1973.0303
- [35] I. Harmati, K. Skrzypczyk, “Robot team coordination for target tracking using fuzzy logic controller in game theoretic framework”, *Robotics and Autonomous System* 57, 75-86, 2009 doi: 10.1016/j.robot.2008.02.004
- [36] R.C. Luo, T.M. Chen, “Target tracking by grey prediction theory and look-ahead fuzzy logic control”, *Proceedings of the 1999 IEEE International Conference on Robotics & Automation, Detroit, Michigan*, 1176-1181, 1999 doi: 10.1109/ROBOT.1999.772521
- [37] S. McGinnity, G.W. Irwin, “Fuzzy logic approach to manoeuvring target tracking”, *IEEE Proceedings- Radar, Sonar and Navigation* 145(6), 337-341, 1998 doi: 10.1049/ip-rsn:19982427
- [38] A. Latif, K. Shankar, P.T. Nguyen, “Legged fire fighter robot movement using PID”, *Journal of Robotics and Control* 1(1), 15-18, 2020 doi: 10.18196/jrc.1104
- [39] C. Semini, N.G. Tsagarakis, B. Vanderborcht, Y. Yang, D.G. Caldwell, “HyQ- Hydraulically Actuated Quadruped Robot: Hopping Leg Prototype”, *Proceedings of the 2nd Biennial IEEE/RAS-EMBS International Conference on Biomedical Robotics and Biomechanics, Scottsdale, USA*, 19-22, 2008 doi: 10.1109/BIOROB.2008.4762913
- [40] A. Patwardhan, A. Prakash, R.G. Chittawadigi, “Kinematic analysis and development of simulation software for nex dexter robotic manipulator”, *Procedia Computer Science* 133, 660-667, 2018 doi: 10.1016/j.procs.2018.07.101
- [41] J. Denavit, R.S. Hartenberg, “A kinematic notation for Lower-pair mechanisms based on matrices”, *ASME Jappl. Mechan.*, 215-221, 1955

- [42] J.R. Schilling, “Fundamentals of Robotics and analysis and control”, *Prentice Hall of India, New Delhi*, 2003
- [43] Ibrahim, K., Sharkawy, A.B: “A hybrid PID control scheme for flexible joint manipulators and a comparison with sliding mode control”, *Ain Shams Engineering Journal* 9, 3451-3457, 2018 doi: 10.1016/j.asej.2018.01.004
- [44] Aström JK, Hägglund T., “PID Controllers: Theory, Design”, and Tuning, *Instrument Society of America, USA*, 70, 1995
- [45] Kim, H.K., Won, D., Kwon, O., Kim, T.J., Kim, S.S., Park, S: “Foot trajectory generation of hydraulic quadruped robots on uneven terrain”, *Proceedings of the 17th World Congress the International Federation of Automatic Control Seoul, Korea*, 3021-3026, 2008 doi: 10.3182/20080706-5-KR-1001.1846
- [46] Aoi, S., Katayama, D., Fujiki, S., Tomita, N., Funato, T., Yamashita, T., Senda, K., Tsuchiya, K: “A stability-based mechanism for hysteresis in the walk-trot transition in quadruped locomotion”, *Journal of The Royal Society*, 10, 1-12, 2013. doi: 10.1098/rsif.2012.0908
- [47] Liu, Q., Chen, X., Han, B., Luo, Z., Luo, X: “Virtual constraint based control of bounding gait of quadruped robots”, *Journal of Bionic Engineering*, 14, 218-231, 2017 doi: 10.1016/S1672-6529(16)60393-1
- [48] M. Hacimurtazaoğlu, “Locking application with fuzzy logic”, *Conference of Academic Information, Akdeniz University* 15, 642-647, 2013
- [49] Y.J. Wang, “Constant force feedback controller design using PID-like fuzzy technique for tapping mode atomic force microscopes”, *Intelligent Control and Automation* 4, 263-279, 2013 doi: 10.1109/CCDC.2009.5192264
- [50] F. Yıldırım, “The effect of geometric changes of propellants which used in large caliber weapons on barrel pressure and muzzle velocity”, *Master Thesis – Ankara University, Ankara, Turkey*, 5-6, 2013
- [51] <http://www.millisavunma.com/mkek-hafif-ve-agir-muhimmat-alesi/>, (last update) 21.01.2017, 18:48 (2017)
- [52] J.R. Rice, “Numerical methods, software and analysis”, *Mc-Graw Hill, New York*, 1983

Appendices

1.

$$x_1 = x - \frac{l_g}{2} \cos \theta + l_1 \cos \theta_1 \quad (\text{a1.1})$$

$$y_1 = y - \frac{l_g}{2} \sin \theta + l_1 \sin \theta_1 \quad (\text{a1.2})$$

$$x_2 = x + \frac{l_g}{2} \cos \theta + l_2 \cos \theta_2 \quad (\text{a1.3})$$

$$y_2 = y + \frac{l_g}{2} \sin \theta + l_2 \sin \theta_2 \quad (\text{a1.4})$$

$$x_3 = x - \frac{l_g}{2} \cos \theta + l_1 \cos \theta_1 + l_3 \cos(\theta_1 + \theta_3) \quad (\text{a1.5})$$

$$y_3 = y - \frac{l_g}{2} \sin \theta + l_1 \sin \theta_1 + l_3 \sin(\theta_1 + \theta_3) \quad (\text{a1.6})$$

$$x_4 = x + \frac{l_g}{2} \cos \theta + l_2 \cos \theta_2 + l_4 \cos(\theta_2 + \theta_4) \quad (\text{a1.7})$$

$$y_4 = y + \frac{l_g}{2} \sin \theta + l_2 \sin \theta_2 + l_4 \sin(\theta_2 + \theta_4) \quad (\text{a1.8})$$

$$x_5 = x - \frac{l_g}{2} \cos \theta + l_5 \cos \theta_5 \quad (\text{a1.9})$$

$$y_5 = y - \frac{l_g}{2} \sin \theta + l_5 \sin \theta_5 \quad (\text{a1.10})$$

$$x_6 = x + \frac{l_g}{2} \cos \theta + l_6 \cos \theta_6 \quad (\text{a1.11})$$

$$y_6 = y + \frac{l_g}{2} \sin \theta + l_6 \sin \theta_6 \quad (\text{a1.12})$$

$$x_7 = x - \frac{l_g}{2} \cos \theta + l_5 \cos \theta_5 + l_7 \cos(\theta_5 + \theta_7) \quad (\text{a1.13})$$

$$y_7 = y - \frac{l_g}{2} \sin \theta + l_5 \sin \theta_5 + l_7 \sin(\theta_5 + \theta_7) \quad (\text{a1.14})$$

$$x_8 = x + \frac{l_g}{2} \cos \theta + l_6 \cos \theta_6 + l_8 \cos(\theta_6 + \theta_8) \quad (\text{a1.15})$$

$$y_8 = y + \frac{l_g}{2} \sin \theta + l_6 \sin \theta_6 + l_8 \sin(\theta_6 + \theta_8) \quad (\text{a1.16})$$

$$x_n = x - a \sin \theta + b \cos(\alpha + \theta) \quad (\text{a1.17})$$

$$y_n = y + a \cos \theta + b \sin(\alpha + \theta) \quad (\text{al.18})$$

2.

$$\begin{aligned}
L = & \frac{1}{2}M\dot{x}^2 + \frac{1}{2}M\dot{y}^2 + \frac{1}{2}I\dot{\theta}^2 + \frac{m_1\dot{x}^2}{2} + \frac{m_1\dot{y}^2}{2} + \frac{m_1l_g^2\dot{\theta}^2}{8} + \frac{m_1l_1^2\dot{\theta}_1^2}{2} + \frac{m_1l_g\dot{x}\dot{\theta}\sin\theta}{2} - m_1\dot{x}l_1\dot{\theta}_1\sin\theta_1 - \frac{m_1l_g\dot{y}\dot{\theta}\cos\theta}{2} \\
& + m_1\dot{y}l_1\dot{\theta}_1\cos\theta_1 - \frac{m_1l_gl_1\dot{\theta}\dot{\theta}_1\cos(\theta-\theta_1)}{2} + \frac{m_2\dot{x}^2}{2} + \frac{m_2\dot{y}^2}{2} + \frac{m_2l_g^2\dot{\theta}^2}{8} + \frac{m_2l_2^2\dot{\theta}_2^2}{2} - \frac{m_2l_g\dot{x}\dot{\theta}\sin\theta}{2} - m_2\dot{x}l_2\dot{\theta}_2\sin\theta_2 \\
& + m_2\dot{y}l_2\dot{\theta}_2\cos\theta_2 + \frac{m_2l_g\dot{y}\dot{\theta}\cos\theta}{2} + \frac{m_2l_gl_2\dot{\theta}\dot{\theta}_2\cos(\theta-\theta_2)}{2} + \frac{m_3\dot{x}^2}{2} + \frac{m_3\dot{y}^2}{2} + \frac{m_3l_g^2\dot{\theta}^2}{8} + \frac{m_3l_1^2\dot{\theta}_1^2}{2} + \frac{m_3l_3^2(\dot{\theta}_1+\dot{\theta}_3)^2}{2} \\
& + \frac{m_3l_g\dot{x}\dot{\theta}\sin\theta}{2} - m_3\dot{x}l_1\dot{\theta}_1\sin\theta_1 - m_3\dot{x}l_3(\dot{\theta}_1+\dot{\theta}_3)\sin(\theta_1+\theta_3) + m_3\dot{y}l_1\dot{\theta}_1\cos\theta_1 - \frac{m_3l_g\dot{y}\dot{\theta}\cos\theta}{2} \\
& + m_3\dot{y}l_3(\dot{\theta}_1+\dot{\theta}_3)\cos(\theta_1+\theta_3) - \frac{m_3l_gl_1\dot{\theta}\dot{\theta}_1\cos(\theta-\theta_1)}{2} - \frac{m_3l_gl_3\dot{\theta}(\dot{\theta}_1+\dot{\theta}_3)\cos(\theta-\theta_1-\theta_3)}{2} + m_3l_1l_3\dot{\theta}_1(\dot{\theta}_1+\dot{\theta}_3)\cos\theta_3 \\
& + \frac{m_4\dot{x}^2}{2} + \frac{m_4\dot{y}^2}{2} + \frac{m_4l_g^2\dot{\theta}^2}{8} + \frac{m_4l_2^2\dot{\theta}_2^2}{2} + \frac{m_4l_4^2(\dot{\theta}_2+\dot{\theta}_4)^2}{2} - \frac{m_4l_g\dot{x}\dot{\theta}\sin\theta}{2} - m_4\dot{x}l_4(\dot{\theta}_2+\dot{\theta}_4)\sin(\theta_2+\theta_4) - m_4\dot{x}l_2\dot{\theta}_2\sin\theta_2 \\
& + \frac{m_4l_g\dot{y}\dot{\theta}\cos\theta}{2} + \frac{m_4l_gl_2\dot{\theta}\dot{\theta}_2\cos(\theta-\theta_2)}{2} + \frac{m_4l_gl_4\dot{\theta}(\dot{\theta}_2+\dot{\theta}_4)\cos(\theta-\theta_2-\theta_4)}{2} + m_4l_2l_4\dot{\theta}_2(\dot{\theta}_2+\dot{\theta}_4)\cos\theta_4 + \frac{m_5\dot{x}^2}{2} + \frac{m_5\dot{y}^2}{2} \\
& + \frac{m_5l_g^2\dot{\theta}^2}{8} + \frac{m_5l_5^2\dot{\theta}_5^2}{2} + \frac{m_5l_g\dot{x}\dot{\theta}\sin\theta}{2} - \frac{m_5l_g\dot{y}\dot{\theta}\cos\theta}{2} - m_5\dot{x}l_5\dot{\theta}_5\sin\theta_5 + m_5\dot{y}l_5\dot{\theta}_5\cos\theta_5 - \frac{m_5l_gl_5\dot{\theta}\dot{\theta}_5\cos(\theta-\theta_5)}{2} + \frac{m_6\dot{x}^2}{2} \\
& + \frac{m_6\dot{y}^2}{2} + \frac{m_6l_g^2\dot{\theta}^2}{8} + \frac{m_6l_6^2\dot{\theta}_6^2}{2} - \frac{m_6l_g\dot{x}\dot{\theta}\sin\theta}{2} - m_6\dot{x}l_6\dot{\theta}_6\sin\theta_6 + \frac{m_6l_g\dot{y}\dot{\theta}\cos\theta}{2} + m_6\dot{y}l_6\dot{\theta}_6\cos\theta_6 + \frac{m_7\dot{x}^2}{2} + \frac{m_7\dot{y}^2}{2} \\
& + \frac{m_7l_g^2\dot{\theta}^2}{8} + \frac{m_7l_5^2\dot{\theta}_5^2}{2} + \frac{m_7l_7^2(\dot{\theta}_5+\dot{\theta}_7)^2}{2} - m_7\dot{x}l_5\dot{\theta}_5\sin\theta_5 - m_7\dot{x}l_7(\dot{\theta}_5+\dot{\theta}_7)\sin(\theta_5+\theta_7) + \frac{m_7l_g\dot{x}\dot{\theta}\sin\theta}{2} - \frac{m_7l_g\dot{y}\dot{\theta}\cos\theta}{2} \\
& + m_7\dot{y}l_5\dot{\theta}_5\cos\theta_5 + m_7\dot{y}l_7(\dot{\theta}_5+\dot{\theta}_7)\cos(\theta_5+\theta_7) - \frac{m_7l_gl_5\dot{\theta}\dot{\theta}_5\cos(\theta-\theta_5)}{2} - \frac{m_7l_gl_7\dot{\theta}(\dot{\theta}_5+\dot{\theta}_7)\cos(\theta-\theta_5-\theta_7)}{2} \\
& + m_7l_5l_7\dot{\theta}_5(\dot{\theta}_5+\dot{\theta}_7)\cos\theta_7 + \frac{m_8\dot{x}^2}{2} + \frac{m_8\dot{y}^2}{2} + \frac{m_8l_g^2\dot{\theta}^2}{8} + \frac{m_8l_6^2\dot{\theta}_6^2}{2} + \frac{m_8l_8^2(\dot{\theta}_6+\dot{\theta}_8)^2}{2} - \frac{m_8l_g\dot{x}\dot{\theta}\sin\theta}{2} - m_8\dot{x}l_6\dot{\theta}_6\sin\theta_6 \\
& + \frac{m_8l_g\dot{y}\dot{\theta}\cos\theta}{2} + m_8\dot{y}l_6\dot{\theta}_6\cos\theta_6 + m_8\dot{y}l_8(\dot{\theta}_6+\dot{\theta}_8)\cos(\theta_6+\theta_8) + m_8l_6l_8\dot{\theta}_6(\dot{\theta}_6+\dot{\theta}_8)\cos\theta_8 + \frac{m_8l_gl_6\dot{\theta}\dot{\theta}_6\cos(\theta-\theta_6)}{2} \\
& + \frac{m_8l_gl_8\dot{\theta}(\dot{\theta}_6+\dot{\theta}_8)\cos(\theta-\theta_6-\theta_8)}{2} + \frac{m_n\dot{x}^2}{2} + \frac{m_n\dot{y}^2}{2} + \frac{m_n a^2 \dot{\theta}^2}{2} + \frac{m_n b^2 (\dot{\alpha} + \dot{\theta})^2}{2} - m_n \dot{x} a \dot{\theta} \cos \theta - m_n \dot{y} a \dot{\theta} \sin \theta \\
& - m_n \dot{x} b (\dot{\alpha} + \dot{\theta}) \sin(\alpha + \theta) + m_n \dot{y} b (\dot{\alpha} + \dot{\theta}) \cos(\alpha + \theta) + m_n a b \dot{\theta} (\dot{\alpha} + \dot{\theta}) \sin \alpha - M g y - m_1 g y + m_1 g \frac{l_g}{2} \sin \theta \\
& - m_1 g l_1 \sin \theta_1 - m_2 g y - m_2 g \frac{l_g}{2} \sin \theta - m_2 g l_2 \sin \theta_2 - m_3 g y + m_3 g \frac{l_g}{2} \sin \theta - m_3 g l_1 \sin \theta_1 - m_3 g l_3 \sin(\theta_1 + \theta_3) \\
& - m_4 g y + m_4 g \frac{l_g}{2} \sin \theta - m_4 g l_2 \sin \theta_2 - m_4 g l_2 \sin(\theta_2 + \theta_4) - m_5 g y + m_5 g \frac{l_g}{2} \sin \theta - m_5 g l_5 \sin \theta_5 - m_6 g y \\
& - m_6 g \frac{l_g}{2} \sin \theta - m_6 g l_6 \sin \theta_6 - m_7 g y + m_7 g \frac{l_g}{2} \sin \theta - m_7 g l_5 \sin \theta_5 - m_7 g l_7 \sin(\theta_5 + \theta_7) - m_8 g y + m_8 g \frac{l_g}{2} \sin \theta \\
& - m_8 g l_8 \sin \theta_8 - m_n g y - m_n g a \cos \theta - m_n g a \sin(\alpha + \theta)
\end{aligned}$$

3.

$$\begin{aligned}
\Sigma F_x = & M\ddot{x} + m_1\ddot{x} + \frac{m_1l_g\ddot{\theta}\sin\theta}{2} + \frac{m_1l_g\dot{\theta}^2\cos\theta}{2} - m_1l_1\ddot{\theta}_1\sin\theta_1 - m_1l_1\dot{\theta}_1^2\cos\theta_1 + m_2\ddot{x} - \frac{m_2l_g\ddot{\theta}\sin\theta}{2} - \frac{m_2l_g\dot{\theta}^2\cos\theta}{2} \\
& - m_2l_2\ddot{\theta}_2\sin\theta_2 - m_2l_2\dot{\theta}_2^2\cos\theta_2 + m_3\ddot{x} + \frac{m_3l_g\ddot{\theta}\sin\theta}{2} + \frac{m_3l_g\dot{\theta}^2\cos\theta}{2} - m_3l_1\ddot{\theta}_1\sin\theta_1 - m_3l_1\dot{\theta}_1^2\cos\theta_1 \\
& - m_3l_3(\ddot{\theta}_1 + \ddot{\theta}_3)\sin(\theta_1 + \theta_3) - m_3l_3(\dot{\theta}_1 + \dot{\theta}_3)^2\cos(\theta_1 + \theta_3) + m_4\ddot{x} - \frac{m_4l_g\ddot{\theta}\sin\theta}{2} - \frac{m_4l_g\dot{\theta}^2\cos\theta}{2} - m_4l_2\ddot{\theta}_2\sin\theta_2 \\
& - m_4l_2\dot{\theta}_2^2\cos\theta_2 - m_4l_4(\ddot{\theta}_2 + \ddot{\theta}_4)\sin(\theta_2 + \theta_4) - m_4l_4(\dot{\theta}_2 + \dot{\theta}_4)^2\cos(\theta_2 + \theta_4) + m_5\ddot{x} + \frac{m_5l_g\ddot{\theta}\sin\theta}{2} \\
& + \frac{m_5l_g\dot{\theta}^2\cos\theta}{2} - m_5l_5\ddot{\theta}_5\sin\theta_5 - m_5l_5\dot{\theta}_5^2\cos\theta_5 + m_6\ddot{x} - \frac{m_6l_g\ddot{\theta}\sin\theta}{2} - \frac{m_6l_g\dot{\theta}^2\cos\theta}{2} - m_6l_6\ddot{\theta}_6\sin\theta_6 \\
& - m_6l_6\dot{\theta}_6^2\cos\theta_6 + m_7\ddot{x} + \frac{m_7l_g\ddot{\theta}\sin\theta}{2} + \frac{m_7l_g\dot{\theta}^2\cos\theta}{2} - m_7l_5\ddot{\theta}_5\sin\theta_5 - m_7l_5\dot{\theta}_5^2\cos\theta_5 \\
& - m_7l_7(\ddot{\theta}_5 + \ddot{\theta}_7)\sin(\theta_5 + \theta_7) - m_7l_7(\dot{\theta}_5 + \dot{\theta}_7)^2\cos(\theta_5 + \theta_7) + m_8\ddot{x} - m_8l_6\ddot{\theta}_6\sin\theta_6 - m_8l_6\dot{\theta}_6^2\cos\theta_6 \\
& - m_8l_8(\ddot{\theta}_6 + \ddot{\theta}_8)\sin(\theta_6 + \theta_8) - \frac{m_8l_g\ddot{\theta}\sin\theta}{2} - \frac{m_8l_g\dot{\theta}^2\cos\theta}{2} - m_8l_8(\dot{\theta}_6 + \dot{\theta}_8)^2\cos(\theta_6 + \theta_8) + m_n\ddot{x} \\
& - m_n a \ddot{\theta} \cos \theta + m_n a \dot{\theta}^2 \sin \theta - m_n b (\ddot{\alpha} + \ddot{\theta}) \sin(\alpha + \theta) - m_n b (\dot{\alpha} + \dot{\theta})^2 \cos(\alpha + \theta)
\end{aligned}$$

$$\Sigma F_y = M\ddot{y} + m_1\ddot{y} - \frac{m_1l_g\ddot{\theta}\cos\theta}{2} + \frac{m_1l_g\dot{\theta}^2\sin\theta}{2} + m_1l_1\ddot{\theta}_1\cos\theta_1 - m_1l_1\dot{\theta}_1^2\sin\theta_1 + m_2\ddot{y} + \frac{m_2l_g\ddot{\theta}\cos\theta}{2} - \frac{m_2l_g\dot{\theta}^2\sin\theta}{2}$$

$$\begin{aligned}
& +m_2l_2\ddot{\theta}_2 \cos \theta_2 - m_2l_2\dot{\theta}_2^2 \sin \theta_2 + m_3\ddot{y} - \frac{m_3l_g\ddot{\theta} \cos \theta}{2} + \frac{m_3l_g\dot{\theta}^2 \sin \theta}{2} + m_3l_1\ddot{\theta}_1 \cos \theta_1 - m_3l_1\dot{\theta}_1^2 \sin \theta_1 \\
& + m_3l_3(\ddot{\theta}_1 + \ddot{\theta}_3) \cos(\theta_1 + \theta_3) - m_3l_3(\dot{\theta}_1 + \dot{\theta}_3)^2 \sin(\theta_1 + \theta_3) + m_4\ddot{y} + \frac{m_4l_g\ddot{\theta} \cos \theta}{2} - \frac{m_4l_g\dot{\theta}^2 \sin \theta}{2} \\
& + m_4l_2\ddot{\theta}_2 \cos \theta_2 - m_4l_2\dot{\theta}_2^2 \sin \theta_2 + m_4l_4(\ddot{\theta}_2 + \ddot{\theta}_4) \cos(\theta_2 + \theta_4) - m_4l_4(\dot{\theta}_2 + \dot{\theta}_4)^2 \sin(\theta_2 + \theta_4) + m_5\ddot{y} \\
& - \frac{m_5l_g\ddot{\theta} \cos \theta}{2} + \frac{m_5l_g\dot{\theta}^2 \sin \theta}{2} + m_5l_5\ddot{\theta}_5 \cos \theta_5 - m_5l_5\dot{\theta}_5^2 \sin \theta_5 + m_6\ddot{y} + \frac{m_6l_g\ddot{\theta} \cos \theta}{2} - \frac{m_6l_g\dot{\theta}^2 \sin \theta}{2} \\
& + m_6l_6\ddot{\theta}_6 \cos \theta_6 - m_6l_6\dot{\theta}_6^2 \sin \theta_6 + m_7\ddot{y} + m_7l_5\ddot{\theta}_5 \cos \theta_5 - m_7l_5\dot{\theta}_5^2 \sin \theta_5 + m_7l_7(\ddot{\theta}_5 + \ddot{\theta}_7) \cos(\theta_5 + \theta_7) \\
& - \frac{m_7l_g\ddot{\theta} \cos \theta}{2} + \frac{m_7l_g\dot{\theta}^2 \sin \theta}{2} - m_7l_7(\dot{\theta}_5 + \dot{\theta}_7)^2 \sin(\theta_5 + \theta_7) + m_8\ddot{y} + \frac{m_8l_g\ddot{\theta} \cos \theta}{2} - \frac{m_8l_g\dot{\theta}^2 \sin \theta}{2} \\
& + m_8l_6\ddot{\theta}_6 \cos \theta_6 - m_8l_6\dot{\theta}_6^2 \sin \theta_6 + m_8l_8(\ddot{\theta}_6 + \ddot{\theta}_8) \cos(\theta_6 + \theta_8) - m_8l_8(\dot{\theta}_6 + \dot{\theta}_8)^2 \sin(\theta_6 + \theta_8) + m_n\ddot{y} \\
& - m_n a \ddot{\theta} \sin \theta - m_n a \dot{\theta}^2 \cos \theta + m_n b (\ddot{\alpha} + \ddot{\theta}) \cos(\alpha + \theta) - m_n b (\dot{\alpha} + \dot{\theta})^2 \sin(\alpha + \theta) + Mg + m_1g + m_2g \\
& + m_3g + m_4g + m_5g + m_6g + m_7g + m_8g + m_n g
\end{aligned}$$

$$\begin{aligned}
\tau = & I\ddot{\theta} + \frac{m_1l_g^2\ddot{\theta}}{4} + \frac{m_1l_g\ddot{x} \sin \theta}{2} - \frac{m_1l_g\ddot{y} \cos \theta}{2} - \frac{m_1l_gl_1\dot{\theta}_1 \cos(\theta - \theta_1)}{2} + \frac{m_1l_gl_1\dot{\theta}_1(\dot{\theta} - \dot{\theta}_1) \sin(\theta - \theta_1)}{2} + \frac{m_2l_g^2\ddot{\theta}}{4} - \frac{m_2l_g\ddot{x} \sin \theta}{2} \\
& + \frac{m_2l_g\ddot{y} \cos \theta}{2} + \frac{m_2l_gl_2\ddot{\theta}_2 \cos(\theta - \theta_2)}{2} - \frac{m_2l_gl_2\dot{\theta}_2(\dot{\theta} - \dot{\theta}_2) \sin(\theta - \theta_2)}{2} + \frac{m_3l_g^2\ddot{\theta}}{4} + \frac{m_3l_g\ddot{x} \sin \theta}{2} + \frac{m_3l_gl_3\dot{\theta}_1(\dot{\theta} - \dot{\theta}_1) \sin(\theta - \theta_1)}{2} \\
& - \frac{m_3l_gl_3(\dot{\theta}_1 + \dot{\theta}_3) \cos(\theta - \theta_1 - \theta_3)}{2} + \frac{m_3l_gl_3(\dot{\theta}_1 + \dot{\theta}_3)(\dot{\theta} - \dot{\theta}_1 - \dot{\theta}_3) \sin(\theta - \theta_1 - \theta_3)}{2} + \frac{m_4l_g^2\ddot{\theta}}{4} - \frac{m_4l_g\ddot{x} \sin \theta}{2} + \frac{m_4l_g\ddot{y} \cos \theta}{2} \\
& + \frac{m_4l_gl_2\ddot{\theta}_2 \cos(\theta - \theta_2)}{2} - \frac{m_4l_gl_2\dot{\theta}_2(\dot{\theta} - \dot{\theta}_2) \sin(\theta - \theta_2)}{2} + \frac{m_4l_gl_4(\ddot{\theta}_2 + \ddot{\theta}_4) \cos(\theta - \theta_2 - \theta_4)}{2} + \frac{m_5l_g^2\ddot{\theta}}{4} + \frac{m_5l_g\ddot{x} \sin \theta}{2} \\
& - \frac{m_4l_gl_4(\dot{\theta}_2 + \dot{\theta}_4)(\dot{\theta} - \dot{\theta}_2 - \dot{\theta}_4) \sin(\theta - \theta_2 - \theta_4)}{2} - \frac{m_5l_g\ddot{y} \cos \theta}{2} - \frac{m_5l_gl_5\dot{\theta}_5 \cos(\theta - \theta_5)}{2} + \frac{m_5l_gl_5\dot{\theta}_5(\dot{\theta} - \dot{\theta}_5) \sin(\theta - \theta_5)}{2} + \frac{m_6l_g^2\ddot{\theta}}{4} \\
& - \frac{m_6l_g\ddot{x} \sin \theta}{2} + \frac{m_6l_g\ddot{y} \cos \theta}{2} + \frac{m_6l_gl_6\dot{\theta}_6 \cos(\theta - \theta_6)}{2} - \frac{m_6l_gl_6\dot{\theta}_6(\dot{\theta} - \dot{\theta}_6) \sin(\theta - \theta_6)}{2} + \frac{m_7l_g^2\ddot{\theta}}{4} + \frac{m_7l_g\ddot{x} \sin \theta}{2} \\
& - \frac{m_7l_g\ddot{y} \cos \theta}{2} - \frac{m_7l_gl_5\dot{\theta}_5 \cos(\theta - \theta_5)}{2} + \frac{m_7l_gl_7\dot{\theta}_5(\dot{\theta} - \dot{\theta}_5) \sin(\theta - \theta_5)}{2} - \frac{m_7l_gl_7(\dot{\theta}_5 + \dot{\theta}_7) \cos(\theta - \theta_5 - \theta_7)}{2} \\
& + \frac{m_7l_gl_7(\dot{\theta}_5 + \dot{\theta}_7)(\dot{\theta} - \dot{\theta}_5 - \dot{\theta}_7) \sin(\theta - \theta_5 - \theta_7)}{2} + \frac{m_8l_g^2\ddot{\theta}}{4} - \frac{m_8l_g\ddot{x} \sin \theta}{2} + \frac{m_8l_g\ddot{y} \cos \theta}{2} + \frac{m_8l_gl_6\dot{\theta}_6 \cos(\theta - \theta_6)}{2} \\
& - \frac{m_8l_gl_6\dot{\theta}_6(\dot{\theta} - \dot{\theta}_6) \sin(\theta - \theta_6)}{2} + \frac{m_8l_gl_8(\ddot{\theta}_6 + \ddot{\theta}_8) \cos(\theta - \theta_6 - \theta_8)}{2} - \frac{m_8l_gl_8(\dot{\theta}_6 + \dot{\theta}_8)(\dot{\theta} - \dot{\theta}_6 - \dot{\theta}_8) \sin(\theta - \theta_6 - \theta_8)}{2} \\
& - \frac{m_1l_gl_1\dot{\theta}_1 \sin(\theta - \theta_1)}{2} + \frac{m_2l_gl_2\dot{\theta}_2 \sin(\theta - \theta_2)}{2} - \frac{m_3l_gl_1\dot{\theta}_1 \sin(\theta - \theta_1)}{2} - \frac{m_3l_gl_3\dot{\theta}_1(\dot{\theta}_1 + \dot{\theta}_3) \sin(\theta - \theta_1 - \theta_3)}{2} \\
& + \frac{m_4l_gl_2\dot{\theta}_2 \sin(\theta - \theta_2)}{2} + \frac{m_4l_gl_4\dot{\theta}_4(\dot{\theta}_2 + \dot{\theta}_4) \sin(\theta - \theta_2 - \theta_4)}{2} - \frac{m_5l_gl_5\dot{\theta}_5 \sin(\theta - \theta_5)}{2} + \frac{m_6l_gl_6\dot{\theta}_6 \sin(\theta - \theta_6)}{2} \\
& - \frac{m_7l_gl_5\dot{\theta}_5 \sin(\theta - \theta_5)}{2} - \frac{m_7l_gl_7\dot{\theta}_7(\dot{\theta}_5 + \dot{\theta}_7) \sin(\theta - \theta_5 - \theta_7)}{2} + \frac{m_8l_gl_6\dot{\theta}_6 \sin(\theta - \theta_6)}{2} + \frac{m_8l_gl_8\dot{\theta}_8(\dot{\theta}_6 + \dot{\theta}_8) \sin(\theta - \theta_6 - \theta_8)}{2} \\
& + m_n a^2 \ddot{\theta} + m_n b^2 \ddot{\theta} + m_n b^2 \ddot{\alpha} - m_n \ddot{x} a \cos \theta - m_n \ddot{x} b \sin(\alpha + \theta) - m_n \ddot{y} a \sin \theta + m_n \ddot{y} b \cos(\alpha + \theta) + m_n \ddot{\alpha} a b \sin \alpha \\
& + m_n a b \dot{\alpha}^2 \cos \alpha + 2m_n a b \dot{\theta} \sin \alpha + 2m_n a b \dot{\theta} \dot{\alpha} \cos \alpha - m_1g \frac{l_g}{2} \cos \theta + m_2g \frac{l_g}{2} \cos \theta - m_3g \frac{l_g}{2} \cos \theta + m_4g \frac{l_g}{2} \cos \theta \\
& - m_5g \frac{l_g}{2} \cos \theta + m_6g \frac{l_g}{2} \cos \theta - m_7g \frac{l_g}{2} \cos \theta + m_8g \frac{l_g}{2} \cos \theta - m_n g a \sin \theta + m_n g b \cos(\alpha + \theta)
\end{aligned}$$

$$\begin{aligned}
\tau_1 = & m_1l_1^2\ddot{\theta}_1 - m_1l_1\ddot{x} \sin \theta_1 + m_1l_1\ddot{y} \cos \theta_1 - \frac{m_1l_gl_1\dot{\theta} \cos(\theta - \theta_1)}{2} + \frac{m_1l_gl_1\dot{\theta}(\dot{\theta} - \dot{\theta}_1) \sin(\theta - \theta_1)}{2} + m_3l_1^2\ddot{\theta}_1 + m_3l_3^2\ddot{\theta}_3 \\
& + m_3l_3^2\ddot{\theta}_1 - m_3l_1\ddot{x} \sin \theta_1 - m_3l_3\ddot{x} \sin(\theta_1 + \theta_3) + m_3l_1\ddot{y} \cos \theta_1 + m_3l_3\ddot{y} \cos(\theta_1 + \theta_3) - \frac{m_3l_gl_1\dot{\theta} \cos(\theta - \theta_1)}{2} \\
& + \frac{m_1l_gl_1\dot{\theta}(\dot{\theta} - \dot{\theta}_1) \sin(\theta - \theta_1)}{2} - \frac{m_3l_gl_3\dot{\theta} \cos(\theta - \theta_1 - \theta_3)}{2} + \frac{m_3l_gl_3\dot{\theta}(\dot{\theta} - \dot{\theta}_1 - \dot{\theta}_3) \sin(\theta - \theta_1 - \theta_3)}{2} + 2m_3l_1l_3\dot{\theta}_1 \cos \theta_3 \\
& - 2m_3l_1l_3\dot{\theta}_1\dot{\theta}_3 \sin \theta_3 + m_3l_1l_3\dot{\theta}_3 \cos \theta_3 - m_3l_1l_3\dot{\theta}_3^2 \sin \theta_3 + \frac{m_1l_gl_1\dot{\theta}_1 \sin(\theta - \theta_1)}{2} + \frac{m_3l_gl_1\dot{\theta}_1 \sin(\theta - \theta_1)}{2} \\
& + \frac{m_3l_gl_3\dot{\theta}_3(\dot{\theta}_1 + \dot{\theta}_3) \sin(\theta - \theta_1 - \theta_3)}{2} + m_1gl_1 \cos \theta_1 + m_3gl_1 \cos \theta_1 + m_3gl_3 \cos(\theta_1 + \theta_3)
\end{aligned}$$

$$\begin{aligned}
\tau_2 = & m_2l_2^2\ddot{\theta}_2 - m_2l_2\ddot{x} \sin \theta_2 + m_2l_2\ddot{y} \cos \theta_2 + m_4l_2^2\ddot{\theta}_2 + m_4l_4^2\ddot{\theta}_2 + m_4l_2^2\ddot{\theta}_4 - m_4l_2\ddot{x} \sin \theta_2 + \frac{m_2l_gl_2\dot{\theta} \cos(\theta - \theta_2)}{2} \\
& - \frac{m_2l_gl_2\dot{\theta}(\dot{\theta} - \dot{\theta}_2) \sin(\theta - \theta_2)}{2} - m_4l_4\ddot{x} \sin(\theta_2 + \theta_4) + m_4l_2\ddot{y} \cos \theta_2 + m_4l_4\ddot{y} \cos(\theta_2 + \theta_4) + \frac{m_4l_gl_2\dot{\theta} \cos(\theta - \theta_2)}{2} \\
& - \frac{m_4l_gl_2\dot{\theta}(\dot{\theta} - \dot{\theta}_2) \sin(\theta - \theta_2)}{2} + \frac{m_4l_gl_4\dot{\theta} \cos(\theta - \theta_2 - \theta_4)}{2} - \frac{m_4l_gl_4\dot{\theta}(\dot{\theta} - \dot{\theta}_2 - \dot{\theta}_4) \sin(\theta - \theta_2 - \theta_4)}{2} + 2m_4l_2l_4\dot{\theta}_2 \cos \theta_4
\end{aligned}$$

$$-2m_4l_2l_4\dot{\theta}_2\dot{\theta}_4 \sin \theta_4 + m_4l_2l_4\ddot{\theta}_4 \cos \theta_4 - m_4l_2l_4\dot{\theta}_4^2 \sin \theta_4 - \frac{m_2l_g l_2 \dot{\theta} \ddot{\theta}_2 \sin(\theta - \theta_2)}{2} - \frac{m_4l_g l_2 \dot{\theta} \ddot{\theta}_2 \sin(\theta - \theta_2)}{2} - \frac{m_4l_g l_4 \dot{\theta}(\dot{\theta}_2 + \dot{\theta}_4) \sin(\theta - \theta_2 - \theta_4)}{2} + m_2gl_2 \cos \theta_2 + m_4gl_2 \cos \theta_2 + m_4gl_4 \cos(\theta_2 + \theta_4)$$

$$\tau_3 = m_3l_3^2\ddot{\theta}_1 + m_3l_3^2\ddot{\theta}_3 - m_3l_3\ddot{x} \sin(\theta_1 + \theta_3) + m_3l_3\ddot{y} \cos(\theta_1 + \theta_3) - \frac{m_3l_g l_3 \ddot{\theta} \cos(\theta - \theta_1 - \theta_3)}{2} + m_3l_1l_3\ddot{\theta}_1 \cos \theta_3 + \frac{m_3l_g l_3 \dot{\theta}(\dot{\theta} - \dot{\theta}_1 - \dot{\theta}_3) \sin(\theta - \theta_1 - \theta_3)}{2} - m_3l_1l_3\dot{\theta}_1\dot{\theta}_3 \sin \theta_3 + \frac{m_3l_g l_3 \dot{\theta}(\dot{\theta}_1 + \dot{\theta}_3) \sin(\theta - \theta_1 - \theta_3)}{2} + m_3gl_3 \cos(\theta_1 + \theta_3) + m_3l_1l_3\dot{\theta}_1(\dot{\theta}_1 + \dot{\theta}_3) \sin \theta_3$$

$$\tau_4 = m_4l_4^2\ddot{\theta}_2 + m_4l_4^2\ddot{\theta}_4 - m_4l_4\ddot{x} \sin(\theta_2 + \theta_4) + m_4l_4\ddot{y} \cos(\theta_2 + \theta_4) + \frac{m_4l_g l_4 \ddot{\theta} \cos(\theta - \theta_2 - \theta_4)}{2} + m_4l_2l_4\ddot{\theta}_2 \cos \theta_4 - \frac{m_4l_g l_4 \dot{\theta}(\dot{\theta} - \dot{\theta}_2 - \dot{\theta}_4) \sin(\theta - \theta_2 - \theta_4)}{2} - m_4l_2l_4\dot{\theta}_2\dot{\theta}_4 \sin \theta_4 - \frac{m_4l_g l_4 \dot{\theta}(\dot{\theta}_2 + \dot{\theta}_4) \sin(\theta - \theta_2 - \theta_4)}{2} + m_4gl_4 \cos(\theta_2 + \theta_4) + m_4l_2l_4\dot{\theta}_2(\dot{\theta}_2 + \dot{\theta}_4) \sin \theta_4$$

$$\tau_5 = m_5l_5^2\ddot{\theta}_5 - m_5l_5\ddot{x} \sin \theta_5 + m_5l_5\ddot{y} \cos \theta_5 + m_7l_5^2\ddot{\theta}_5 + m_7l_7^2\ddot{\theta}_7 + m_7l_7^2\ddot{\theta}_5 - m_7l_5\ddot{x} \sin \theta_5 - \frac{m_5l_g l_5 \ddot{\theta} \cos(\theta - \theta_5)}{2} + \frac{m_5l_g l_5 \dot{\theta}(\dot{\theta} - \dot{\theta}_5) \sin(\theta - \theta_5)}{2} - m_7l_7\ddot{x} \sin(\theta_5 + \theta_7) + m_7l_5\ddot{y} \cos \theta_5 + m_7l_7\ddot{y} \cos(\theta_5 + \theta_7) - \frac{m_7l_g l_5 \ddot{\theta} \cos(\theta - \theta_5)}{2} + \frac{m_5l_g l_5 \dot{\theta}(\dot{\theta} - \dot{\theta}_5) \sin(\theta - \theta_5)}{2} - \frac{m_7l_g l_7 \dot{\theta} \cos(\theta - \theta_5 - \theta_7)}{2} + \frac{m_7l_g l_7 \dot{\theta}(\dot{\theta} - \dot{\theta}_5 - \dot{\theta}_7) \sin(\theta - \theta_5 - \theta_7)}{2} + 2m_7l_5l_7\ddot{\theta}_5 \cos \theta_7 - 2m_7l_5l_7\dot{\theta}_5\dot{\theta}_7 \sin \theta_7 + m_7l_5l_7\ddot{\theta}_7 \cos \theta_7 - m_7l_5l_7\dot{\theta}_7^2 \sin \theta_7 + \frac{m_5l_g l_5 \dot{\theta} \ddot{\theta}_5 \sin(\theta - \theta_5)}{2} + \frac{m_7l_g l_5 \dot{\theta} \ddot{\theta}_5 \sin(\theta - \theta_5)}{2} + \frac{m_7l_g l_7 \dot{\theta}(\dot{\theta}_5 + \dot{\theta}_7) \sin(\theta - \theta_5 - \theta_7)}{2} + m_5gl_5 \cos \theta_5 + m_7gl_5 \cos \theta_5 + m_7gl_7 \cos(\theta_5 + \theta_7)$$

$$\tau_6 = m_6l_6^2\ddot{\theta}_6 - m_6l_6\ddot{x} \sin \theta_6 + m_6l_6\ddot{y} \cos \theta_6 + m_8l_6^2\ddot{\theta}_6 + m_8l_8^2\ddot{\theta}_6 + m_8l_6^2\ddot{\theta}_8 - m_8l_6\ddot{x} \sin \theta_6 + \frac{m_6l_g l_6 \ddot{\theta} \cos(\theta - \theta_6)}{2} - \frac{m_6l_g l_6 \dot{\theta}(\dot{\theta} - \dot{\theta}_6) \sin(\theta - \theta_6)}{2} - m_8l_8\ddot{x} \sin(\theta_6 + \theta_8) + m_8l_6\ddot{y} \cos \theta_6 + m_8l_8\ddot{y} \cos(\theta_6 + \theta_8) - \frac{m_8l_g l_6 \dot{\theta}(\dot{\theta} - \dot{\theta}_6) \sin(\theta - \theta_6)}{2} + \frac{m_8l_g l_8 \ddot{\theta} \cos(\theta - \theta_6 - \theta_8)}{2} + 2m_8l_6l_8\ddot{\theta}_6 \cos \theta_8 - \frac{m_8l_g l_8 \dot{\theta}(\dot{\theta} - \dot{\theta}_6 - \dot{\theta}_8) \sin(\theta - \theta_6 - \theta_8)}{2} - 2m_8l_6l_8\dot{\theta}_6\dot{\theta}_8 \sin \theta_8 + m_8l_6l_8\ddot{\theta}_8 \cos \theta_8 - m_8l_6l_8\dot{\theta}_8^2 \sin \theta_8 - \frac{m_6l_g l_6 \dot{\theta} \ddot{\theta}_6 \sin(\theta - \theta_6)}{2} - \frac{m_8l_g l_6 \dot{\theta} \ddot{\theta}_6 \sin(\theta - \theta_6)}{2} - \frac{m_8l_g l_8 \dot{\theta}(\dot{\theta}_6 + \dot{\theta}_8) \sin(\theta - \theta_6 - \theta_8)}{2} + m_6gl_6 \cos \theta_6 + m_8gl_6 \cos \theta_6 + m_8gl_8 \cos(\theta_6 + \theta_8)$$

$$\tau_7 = m_7l_7^2\ddot{\theta}_5 + m_7l_7^2\ddot{\theta}_7 - m_7l_7\ddot{x} \sin(\theta_5 + \theta_7) + m_7l_7\ddot{y} \cos(\theta_5 + \theta_7) - \frac{m_7l_g l_7 \ddot{\theta} \cos(\theta - \theta_5 - \theta_7)}{2} + \frac{m_7l_g l_7 \dot{\theta}(\dot{\theta} - \dot{\theta}_5 - \dot{\theta}_7) \sin(\theta - \theta_5 - \theta_7)}{2} + m_7l_5l_7\ddot{\theta}_5 \cos \theta_7 - m_7l_5l_7\dot{\theta}_5\dot{\theta}_7 \sin \theta_7 + \frac{m_7l_g l_7 \dot{\theta}(\dot{\theta}_5 + \dot{\theta}_7) \sin(\theta - \theta_5 - \theta_7)}{2} + m_7l_5l_7\dot{\theta}_5(\dot{\theta}_5 + \dot{\theta}_7) \sin \theta_7 + m_7gl_7 \cos(\theta_5 + \theta_7)$$

$$\tau_8 = m_8l_8^2\ddot{\theta}_6 + m_8l_8^2\ddot{\theta}_8 - m_8l_8\ddot{x} \sin(\theta_6 + \theta_8) + m_8l_8\ddot{y} \cos(\theta_6 + \theta_8) + \frac{m_8l_g l_8 \ddot{\theta} \cos(\theta - \theta_6 - \theta_8)}{2} - \frac{m_8l_g l_8 \dot{\theta}(\dot{\theta} - \dot{\theta}_6 - \dot{\theta}_8) \sin(\theta - \theta_6 - \theta_8)}{2} + m_8l_6l_8\ddot{\theta}_6 \cos \theta_8 - m_8l_6l_8\dot{\theta}_6\dot{\theta}_8 \sin \theta_8 - \frac{m_8l_g l_8 \dot{\theta}(\dot{\theta}_6 + \dot{\theta}_8) \sin(\theta - \theta_6 - \theta_8)}{2} + m_8l_6l_8\dot{\theta}_6(\dot{\theta}_6 + \dot{\theta}_8) \sin \theta_8 + m_8gl_8 \cos(\theta_6 + \theta_8)$$

$$\tau_n = m_nb^2\ddot{\alpha} + m_nb^2\ddot{\theta} - m_nb\ddot{x} \sin(\alpha + \theta) + m_nb\ddot{y} \cos(\alpha + \theta) + m_nab\ddot{\theta} \sin \alpha + m_nab\dot{\theta}\dot{\alpha} \cos \alpha - m_nab\dot{\theta}(\dot{\theta} + \dot{\alpha}) \cos \alpha + m_ngb \cos(\alpha + \theta)$$

4.

$$[J_{R_{shoulder}}] = \begin{bmatrix} 1 & 0 & (-l_g/2) \sin \theta & 0 & 0 & 0 & 0 & 0 & 0 & 0 & 0 \\ 0 & 1 & (l_g/2) \cos \theta & 0 & 0 & 0 & 0 & 0 & 0 & 0 & 0 \end{bmatrix}$$

$$\begin{aligned}
[J_{L_{\text{shoulder}}}] &= \begin{bmatrix} 0 & 0 & (l_g/2) \sin \theta & 0 & 0 & 0 & 0 & 0 & 0 & 0 & 0 & 0 \\ 1 & 1 & (-l_g/2) \cos \theta & 0 & 0 & 0 & 0 & 0 & 0 & 0 & 0 & 0 \end{bmatrix} \\
[J_1] &= \begin{bmatrix} 1 & 0 & (l_g/2) \sin \theta - l_1 \sin \theta_1 & -l_1 \sin \theta_1 & 0 & 0 & 0 & 0 & 0 & 0 & 0 \\ 0 & 1 & (-l_g/2) \cos \theta + l_1 \cos \theta_1 & l_1 \cos \theta_1 & 0 & 0 & 0 & 0 & 0 & 0 & 0 \end{bmatrix} \\
[J_2] &= \begin{bmatrix} 1 & 0 & (-l_g/2) \sin \theta - l_2 \sin \theta_2 & 0 & -l_2 \sin \theta_2 & 0 & 0 & 0 & 0 & 0 & 0 \\ 0 & 1 & (l_g/2) \cos \theta + l_2 \cos \theta_2 & 0 & l_2 \cos \theta_2 & 0 & 0 & 0 & 0 & 0 & 0 \end{bmatrix} \\
[J_3] &= \begin{bmatrix} 1 & 0 & (l_g/2) \sin \theta - l_1 \sin \theta_1 - l_3 \sin(\theta_1 + \theta_3) & -l_1 \sin \theta_1 - l_3 \sin(\theta_1 + \theta_3) & 0 & -l_3 \sin(\theta_1 + \theta_3) & 0 & 0 & 0 & 0 & 0 \\ 0 & 1 & (-l_g/2) \cos \theta + l_1 \cos \theta_1 + l_3 \cos(\theta_1 + \theta_3) & l_1 \cos \theta_1 + l_3 \cos(\theta_1 + \theta_3) & 0 & l_3 \cos(\theta_1 + \theta_3) & 0 & 0 & 0 & 0 & 0 \end{bmatrix} \\
[J_4] &= \begin{bmatrix} 1 & 0 & (-l_g/2) \sin \theta - l_2 \sin \theta_2 - l_4 \sin(\theta_2 + \theta_4) & 0 & -l_2 \sin \theta_2 - l_4 \sin(\theta_2 + \theta_4) & 0 & 0 & -l_4 \sin(\theta_2 + \theta_4) & 0 & 0 & 0 \\ 0 & 1 & (l_g/2) \cos \theta + l_2 \cos \theta_2 + l_4 \cos(\theta_2 + \theta_4) & 0 & l_2 \cos \theta_2 + l_4 \cos(\theta_2 + \theta_4) & 0 & 0 & l_4 \cos(\theta_2 + \theta_4) & 0 & 0 & 0 \end{bmatrix} \\
[J_5] &= \begin{bmatrix} 1 & 0 & (l_g/2) \sin \theta - l_5 \sin \theta_5 & 0 & 0 & 0 & 0 & -l_5 \sin \theta_5 & 0 & 0 & 0 \\ 0 & 1 & (-l_g/2) \cos \theta + l_5 \cos \theta_5 & 0 & 0 & 0 & 0 & l_5 \cos \theta_5 & 0 & 0 & 0 \end{bmatrix} \\
[J_6] &= \begin{bmatrix} 1 & 0 & (-l_g/2) \sin \theta - l_6 \sin \theta_6 & 0 & 0 & 0 & 0 & -l_6 \sin \theta_6 & 0 & 0 \\ 0 & 1 & (l_g/2) \cos \theta + l_6 \cos \theta_6 & 0 & 0 & 0 & 0 & l_6 \cos \theta_6 & 0 & 0 \end{bmatrix} \\
[J_7] &= \begin{bmatrix} 1 & 0 & (l_g/2) \sin \theta - l_5 \sin \theta_5 - l_7 \sin(\theta_5 + \theta_7) & 0 & 0 & 0 & 0 & -l_5 \sin \theta_5 - l_7 \sin(\theta_5 + \theta_7) & 0 & -l_7 \sin(\theta_5 + \theta_7) & 0 \\ 0 & 1 & (-l_g/2) \cos \theta + l_5 \cos \theta_5 + l_7 \cos(\theta_5 + \theta_7) & 0 & 0 & 0 & 0 & l_5 \cos \theta_5 + l_7 \cos(\theta_5 + \theta_7) & 0 & l_7 \cos(\theta_5 + \theta_7) & 0 \end{bmatrix} \\
[J_8] &= \begin{bmatrix} 1 & 0 & (-l_g/2) \sin \theta - l_6 \sin \theta_6 - l_8 \sin(\theta_6 + \theta_8) & 0 & 0 & 0 & 0 & -l_6 \sin \theta_6 - l_8 \sin(\theta_6 + \theta_8) & 0 & -l_8 \sin(\theta_6 + \theta_8) \\ 0 & 1 & (l_g/2) \cos \theta + l_6 \cos \theta_6 + l_8 \cos(\theta_6 + \theta_8) & 0 & 0 & 0 & 0 & l_6 \cos \theta_6 + l_8 \cos(\theta_6 + \theta_8) & 0 & l_8 \cos(\theta_6 + \theta_8) \end{bmatrix}
\end{aligned}$$

5.

$$[J_n] = \begin{bmatrix} 1 & 0 & -a \cos \theta - b \sin(\alpha + \theta) & 0 & 0 & 0 & 0 & 0 & 0 & 0 & 0 & -b \sin(\alpha + \theta) \\ 0 & 1 & -a \sin \theta + b \cos(\alpha + \theta) & 0 & 0 & 0 & 0 & 0 & 0 & 0 & 0 & b \cos(\alpha + \theta) \end{bmatrix}$$